

THE ROLE OF AP-2 $\alpha$  AND AP-2 $\beta$  IN RETINAL DEVELOPMENT

THE ROLE OF AP-2 $\alpha$  AND AP-2 $\beta$  IN AMACRINE CELL DEVELOPMENT AND  
PATTERNING

By

EMILY ANNE HICKS, B.SC. (HONOURS)

A Thesis

Submitted to the School of Graduate Studies

in Partial Fulfillment of the Requirements

for the Degree

Master of Applied Science

McMaster University

©Copyright by Emily Anne Hicks, May 2017

M.A.Sc. Thesis – EA. Hicks; McMaster University – Biomedical Engineering

MASTER OF APPLIED SCIENCE (2017)  
(Biomedical Engineering)

McMaster University  
Hamilton, Ontario

TITLE: The Role of AP-2 $\alpha$  and AP-2 $\beta$  in Amacrine Cell  
Development and Patterning

AUTHOR: Emily Anne Hicks, B.Sc. (Honours) (Memorial University)

SUPERVISOR: Dr. Judith A. West-Mays

NUMBER OF PAGES: viii, 78

## ABSTRACT

Previous studies from our lab have shown that Activating protein-2 (AP-2) transcription factors, AP-2 $\alpha$  and AP-2 $\beta$  are important in retinal development, specifically in the developing horizontal and post-mitotic amacrine cells. Conditional deletion of AP-2 $\alpha$  and AP-2 $\beta$  from the retina of mice resulted in a variety of abnormalities including loss of horizontal cells, defects in the photoreceptor ribbons in which synapses failed to form, along with evidence that amacrine cell mosaic patterning may be disrupted. The current thesis examined the neural retina of these AP-2 $\alpha$  and AP-2 $\beta$  conditional mice in greater detail using immunofluorescence of histological sections and whole retinas, and electroretinograms to measure retinal function in post-natal adult mice. Examining regularity of the amacrine cell mosaics of these double mutants showed the loss of AP-2 $\alpha$  and AP-2 $\beta$  led to significant irregularities in the mosaic patterning of these cells as determined by Voronoi domain areas ( $P < 0.01$ ) and nearest-neighbour distances ( $P < 0.03$ ). No significant changes in amacrine population numbers were observed. Observed cellular changes in the double conditional knock out mice were reflected as a change in the retinal response to light as recorded by electroretinograms. For example, the b-wave amplitude, representative of the interneuron signal processing, was significantly affected in those mice lacking AP-2 $\alpha$  and AP-2 $\beta$  ( $P < 0.0001$ ). Taken together, the work presented in this thesis implicates the requirement of AP-2 $\alpha$  and AP-2 $\beta$  for the correct amacrine mosaic patterning and for the proper functional light response in the retina.

## ACKNOWLEDGEMENTS

It is with utmost appreciation and admiration that I extend my gratitude to my supervisor, Dr. Judy West-Mays. You were always there to offer guidance, support, and encouragement over the past three years and I am very thankful to have had the opportunity to be a part of such a wonderful lab environment. Furthermore, many thanks to my committee members, Dr. Bernardo Trigatti and Dr. Mike Noseworthy for your expertise, valuable input, and insightful comments throughout this process, it was greatly appreciated.

I would like to extend a huge, heartfelt thank you to Paula Deschamps. Much of the work in this dissertation would not have been completed without your assistance, especially with the mice. Thank you for your unending patience and for everything you do in the lab. To my current lab mates: Dr. Aftab Taiyab, Dr. Faryan Tayyari, Anna Korol, Scott Bowman, Monica Akula, and Toby Saraco; and former lab-mate Vanessa Martino – It has been an absolute pleasure to work with such a fantastic group of people. Although conversations were not always scientific, they were more often than not a delight. I appreciate this experience which I've been fortunate enough to share with you, thank you for making it a memorable one. I wish you all the best, wherever life may take you.

The past three years have been full of scattered ups and downs, and I have been extremely blessed with fantastic parents, wonderful siblings, and great friends who have supported me through them all. To my friends on the east coast, you may be 3000 km away but you have always been there to provide some much needed stress relief with w(h)ine nights. To my siblings, thank you for paving the road before me. Seeing you succeed in your respective careers has been truly motivating and I hope to learn from your example. Finally, thank you to my parents for your unwavering support, encouragement, and reminding me to “knock ‘em down in the crease”.

## TABLE OF CONTENTS

<b>ABSTRACT</b> .....	iii
<b>ACKNOWLEDGEMENTS</b> .....	iv
<b>LIST OF TABLES &amp; FIGURES</b> .....	vii
<b>LIST OF ABBREVIATIONS</b> .....	viii
<b>CHAPTER ONE – General Introduction.</b> .....	<b>1</b>
1.1 Eye Development in Vertebrates .....	2
1.2 The Vertebrate Retina .....	2
1.2.1 Horizontal and Amacrine Cell Development. ....	4
1.2.2 Mosaic Patterning of Amacrine Cells. ....	7
1.2.3 Electrophysiology of the Retina. ....	9
1.3 Activating Protein-2. ....	10
<b>CHAPTER TWO – Rationale, Main Hypothesis &amp; Research Aims.</b> .....	<b>14</b>
2.1 Rationale for Study .....	15
2.2 Main Hypothesis .....	16
2.3 Specific Aims .....	16
2.3.1 Examine and analyze the amacrine cell spacing in conditional knockout mice .....	16
2.3.2 Examine retinal function in conditional knockout mouse models. ....	17
2.3.3 Understand the genetic cascade for amacrine cell development. ....	17
<b>CHAPTER THREE – Experimental Design</b> .....	<b>18</b>
3.1 Generation of Mouse Lines .....	19
3.2 Histology .....	20
3.3 Immunofluorescence .....	21
3.4 Cell Counting Studies .....	21
3.5 Flat Mount Retinas .....	22
3.6 Electroretinograms .....	23

<b>CHAPTER FOUR - Results.</b> . . . . .	<b>27</b>
4.1 Generation of <i>Tcfap2a</i> , <i>Tcfap2b</i> , and <i>Tcfap2a/b</i> Conditional KO mice . . . . .	28
4.2 Cholinergic Amacrine Cell Mosaics are Altered by Deletion of AP-2 $\alpha$ and AP-2 $\beta$ from the Retina . . . . .	29
4.3 The Physiological Response to Light is Altered by Loss of AP-2 $\alpha$ and AP-2 $\beta$ from the Retina. . . . .	32
4.4 Amacrine Cell Development is not Dependent on AP-2 $\alpha$ and AP-2 $\beta$ . . . . .	33
<b>CHAPTER FIVE – Discussion.</b> . . . . .	<b>36</b>
5.1 AP-2 $\alpha$ and AP-2 $\beta$ Deletion Leads to Downstream Effects in Amacrine Cell Mosaic Patterning. . . . .	38
5.2 Loss of AP-2 $\alpha$ and AP-2 $\beta$ from the Developing Retina Effects the Physiological Response to Light. . . . .	43
5.3 Conclusions and Future Directions. . . . .	45
<b>REFERENCES.</b> . . . . .	<b>48</b>
<b>FIGURES.</b> . . . . .	<b>56</b>

**LIST OF TABLES & FIGURES**

Table 1. PCR Protocols for Genotyping . . . . .	25
Table 2. List of Antibodies for Immunofluorescence . . . . .	26
Figure 1. The eye. . . . .	57
Figure 2. Vertebrate eye development. . . . .	58
Figure 3. Retinal development. . . . .	59
Figure 4. The transcriptional cascades regulating amacrine and horizontal cell development . . . . .	60
Figure 5. Activating Protein-2. . . . .	61
Figure 6. Generation of double conditional <i>Tcfap2a/Tcfap2b</i> mutants. . . . .	62
Figure 7. Generation of single conditional <i>Tcfap2a</i> and <i>Tcfap2b</i> mutants. . . . .	63
Figure 8. Cre-loxP tissue specific deletion. . . . .	64
Figure 9. Expression of AP-2 $\alpha$ and AP-2 $\beta$ expression in the retina. . . . .	65
Figure 10. Voronoi domain areas and nearest-neighbour distances. . . . .	66
Figure 11. Representative nearest-neighbour distances in single and double KO mouse retinas. . . . .	67
Figure 12. Decreased regulation in nearest-neighbour distances in double conditional KO mice. . . . .	68
Figure 13. Representative Voronoi domain areas in single and double KO mouse retinas. . . . .	69
Figure 14. Decreased Voronoi domain regularity indexes in double conditional KO mice. . . . .	70
Figure 15. Cholinergic amacrine cells in the INL and GCL of conditional KO mice remain unchanged . . . . .	71
Figure 16. Representative dark-adapted, full-field electroretinograms recording. . . . .	72
Figure 17. A-wave amplitude decreases with increasing flash intensities. . . . .	73
Figure 18. B-wave amplitudes are attenuated in double conditional KO electroretinograms. . . . .	74
Figure 19. Expression of GABAergic amacrine cell markers, GAT1 and SOX2. . . . .	75
Figure 20. GABAergic amacrine cells do not significantly decrease in AP-2 $\alpha$ and AP-2 $\beta$ conditional KOs. . . . .	76
Figure 21. Expression of the glycinergic amacrine cell marker, GLYT1 . . . . .	77
Figure 22. Expression of Calretinin in knockout mice. . . . .	78



### LIST OF ABBREVIATIONS

AC	Amacrine cell	Isl1/2	Islet 1/2
$\alpha$ KI	AP-2 $\alpha$ conditional knockout	KO	Knockout
ANOVA	Analysis of variance	MG	Müller glia
AP-2	Activating Protein-2	NGF	Nerve growth factor
ARVO	Association for Research in Vision and Ophthalmology	NN	Nearest-neighbour
BC	Bipolar cell	NNRI	Nearest-neighbour regularity index
bHLH	Basic Helix-loop-Helix	NR	Neural retina
$\beta$ KO	AP-2 $\beta$ conditional knockout	Oc-1	Onecut-1
BOFS	Branchio-Oculo-Facial-Syndrome	ONL	Outer nuclear layer
bp	Base pair	OP	Oscillatory potential
ChAT	Cholinergic acetyltransferase	OPL	Outer plexiform layer
CNS	Central nervous system	P	Post-natal day
CNTF	Ciliary neurotrophic factor	Pax6	Paired box 6
DAPI	4,6-diamino-2-phenylindole	PBS	Phosphate buffered saline
DBL	AP-2 $\alpha$ /AP-2 $\beta$ conditional knockout	PBST	Phosphate buffered saline with TritonX-100
DNA	Deoxyribonucleic acid	PCR	Polymerase chain reaction
DSCAM	Down Syndrome cell adhesion molecule	PGK	Phosphoglycerokinase
E	Embryonic day	PR	Photoreceptor
EGF	Epidermal growth factor	Ptf1a	Pancreas specific transcription factor 1a
ERG	Electroretinogram	Pttg1	Pituitary tumor transforming gene-1
Foxn4	Forkhead box N4	RI	Regularity index
GABA	$\gamma$ -Aminobutyric acid	RPC	Retinal progenitor cell
GAT1	GABA transporter 1	RPE	Retinal pigment epithelium
GC	Ganglion cell	Rx	Retinal homeobox protein
GCL	Ganglion cell layer	SD	Standard deviation
GLYT1	Glycine transporter 1	Shh	Sonic hedgehog
HC	Horizontal cell	Sox2	Sex determining region Y-box 2
HD	Homeodomain	TGF $\alpha$	Transforming growth factor $\alpha$
INL	Inner nuclear layer	VD	Voronoi domain
IPL	Inner plexiform layer	VDRI	Voronoi domain regularity index

**CHAPTER ONE**  
**General Introduction**

## **1.1 Eye Development in Vertebrates**

The vertebrate eye is a highly specialized organ, converting light signals from the environment into a set of electrical signals transmitted to the brain through complex neural pathways (Fig. 1). Proper formation of the eye is carefully maintained through the balance of many biological factors and the co-ordinated development of the forebrain neuroepithelium, periocular mesenchyme, and the surface ectoderm (Chow & Lang, 2001; Cvekl & Tam, 2004). Induction of the optic field begins at gastrulation when the neuroepithelium meets the overlying surface ectoderm (Fig. 2). The diencephalon then evaginates, forming outpockets of neuroepithelium known as the optic vesicles (Martinez-Morales *et al.*, 2004). The optic vesicle then proceeds to invaginate, forming the optic cup, patterned into three domains; the inner neural retina, the outer retinal pigment epithelium and the optic stalk (Bharti *et al.*, 2006). The differentiation into the inner and outer retina occurs when the lens placode pinches off to form the lens vesicle which becomes the transparent lens, allowing light to reach the retina (Chow & Lang, 2001). The cornea is formed from the overlying surface ectoderm (Chow & Lang, 2001).

## **1.2 The Vertebrate Retina**

As the optic cup continues to develop, the outer layer thins as it differentiates into the retinal pigment epithelium (RPE), a monolayer of multifunctional, pigmented cells. The RPE is required for maintenance of the blood-retina-barrier, water and ion flow between the neural retina and the choroid, absorption of stray light, and controlling retinoid metabolism (Bok, 1993). The inner layer proliferates into a multilayered neuroepithelium,

eventually becoming the neural retina (NR). Neural retinogenesis begins at embryonic day (E) 10.5 and continues until post-natal day (P) 11. During this time, multipotent retinal progenitor cells (RPCs) form the six principle neurons, Müller glia, and astrocytes (Marquardt, 2003; Levine *et al.*, 2004). These cells emerge in a fixed, overlapping, chronological order beginning with the ganglion cells (GC) followed by horizontal cells (HC), cone photoreceptors (PR), amacrine cells (AC), rod PR, bipolar cells (BC), and finally the non-neuronal Müller glia (MG), organized into nuclear and plexiform layers (Fig. 3) (Marquardt, 2003; Zhang *et al.*, 2011). This sequence of neural induction in the NR is conserved across species with all vertebrates studied exhibiting the same pattern of cell genesis (Livesey & Cepko., 2001). These cells collectively emerge from the outer surface of the NR then migrate to occupy various fixed positions within the neural retina. Cells born at the same time, such as the HC and AC, can reside in different layers (Wong & Godhino, 2004). Rod and cone PRs reside in the outer nuclear layer (ONL), while the inner nuclear layer (INL) contains the cell bodies of HC, BC, AC, and MG. The ganglion cell layer (GCL), closest to the vitreous humour, has the cell bodies of GC and displaced AC. Connections between the PR, BC, and HC are found in the outer plexiform layer (OPL) while connections between BC, GC, and AC are found in the inner plexiform layer (IPL) (Smith *et al.*, 2002).

There is a range of extrinsic and intrinsic factors, many of which remain unidentified, that control the numerous steps in RPC development; cell-cycle exit, cell fate commitment and differentiation into functional neuron or glia. Transcription factors have emerged as key regulators of these processes. All mitotic RPCs co-express a set of

homeodomain (HD) transcription factors Pax6, Six3, Rx, Vsx2, the basic helix-loop-helix (bHLH) transcription factor Hes1, as well as various inhibitory and excitatory factors TGF $\alpha$ , EGF, Shh, NGF, CNTF (Marquardt, 2003; Li & Dashwood, 2004). Throughout retinal development, some cell lineages continue to express these factors while others become downregulated. Different combinations of factors direct cell fate and differentiation into the various cell types while changing intrinsic properties determine how the cells will respond to these external signals during development (Cepko *et al.*, 1996). Other transcription factors involved include Ptf1a, Math3, Mash1, NeuroD, and AP-2 $\alpha$  and AP-2 $\beta$  expressed in subsets of RPCs (Bassett *et al.*, 2007; 2010; 2012; Jin *et al.*, 2015; Li *et al.*, 2004; West-Mays *et al.*, 1999).

### **1.2.1 Horizontal and Amacrine Cell Development**

Several members within the transcriptional cascades regulating HC and AC specification have been identified (Fig. 4). Foxn4 initiates HC and AC differentiation and activates downstream gene targets required for the birth of these cell types (Xiang, 2013). Loss of *Foxn4* leads to an elimination of both HCs and ACs while causing an excess number of PRs to develop (Li *et al.*, 2004). Foxn4 specifies both HC and AC by regulating the expression of downstream genes such as *Ptf1a*, *Math3*, and *NeuroD* which are essential for their genesis (Xiang & Li, 2013). Ptf1a, a bHLH transcription factor, is required for the generation of HC and most ACs (Fujitani *et al.*, 2006). Both Foxn4 and Ptf1a knockout (KO) retinas are missing the expression of Prox1, an HD factor essential for HC genesis, but not for the formation of other cell types (Dyer *et al.*, 2003). Similarly,

a *Prox1* deletion results in a complete loss of HC without affecting AC genesis (Dyer *et al.*, 2003).

A recent study has identified *Onecut-1* (*Oc-1*) as another essential transcriptional regulator of HC development (Wu *et al.*, 2013). Loss of *Oc-1* in the murine retina results in a complete loss of HC (Wu *et al.*, 2013). *Oc-1* expression is downregulated in *Foxn4* ablated retinas but remains the same in *Ptf1a*<sup>-/-</sup> mutants suggesting *Foxn4* functions upstream of *Oc-1* while *Ptf1a* and *Oc-1* work similarly to specify HC genesis (Wu *et al.*, 2013). Another factor specific to HC is *Lim1*, expressed exclusively in post-mitotic HC in the developing and adult retina (Poche *et al.*, 2007). *Lim1* may not be required for the specification of HCs, but it is imperative for their migration to the correct location within the retina. For example, in *Lim-1* conditional KO mice, the HC are displaced amongst the AC and do not attain the correct morphology (Poche *et al.*, 2007).

Precursor cells that express *Ptf1a* in conjunction with *Prox1* are directed towards an HC fate, while *Ptf1a* cells expressing *Math3* and *NeuroD* are directed towards an AC fate (Dyer *et al.*, 2003; Inoue *et al.*, 2002). The bHLH factors *Math3* and *NeuroD* are both expressed in RPCs as well as in developing HC and AC (Inoue *et al.*, 2002; Trimarchi *et al.*, 2008). *Math3-NeuroD* double mutants show a complete loss of AC while HC population remain unchanged (Inoue *et al.*, 2002). Misexpression of *NeuroD* or *Math3* alone leads to rod PR formation (Hatakeyama *et al.*, 2001; Inoue *et al.*, 2002). However, misexpression of either *Pax6* or *Six3* along with *NeuroD* strongly promotes the generation of AC, while misexpression of *Pax6* or *Sox3* with *Math3* induces both AC and HC formation (Inoue *et al.*, 2002). *Math3* and *NeuroD* are known to act downstream of

*Foxn4*, a forkhead/winged helix transcription factor expressed in mitotic RPCs during AC and HC birth, and is required for the genesis of all HC and vast majority of AC (Li *et al.*, 2004).

The remarkable number of individual AC subtypes suggests the need for an intrinsic regulatory pathway acting downstream of the general AC fate (Poche & Reese, 2009). Considering the diversity of AC, relatively few transcription factors are currently known to have subtype-specific influences (Elshatory *et al.*, 2007). *Barhl2*, a member of the BarH class of homeodomain factors, is expressed in post-mitotic GC, HC, and AC (Mo *et al.*, 2004). Misexpression of *Barhl2* promotes glycinergic AC formation, whereas *Barhl2*<sup>-/-</sup> mice exhibit a loss of both glycinergic and GABAergic AC but a significant increase in cholinergic AC (Mo *et al.*, 2004). Deletion of the *Bhlhb5* causes a reduction of GABAergic amacrine cells (Feng *et al.*, 2006) and *Isl1* is required for differentiation into the cholinergic subtype (Elshatory *et al.*, 2007). *Ptf1a* has been shown to be a critical regulator for differentiation of HC and AC. *Tcfap2a* and *Tcfap2b* are two major downstream effectors of *Ptf1a*, with a significant decrease of their transcripts in *Ptf1a* null mice (Jin *et al.*, 2015). Overexpression of these two transcription factors mimics that of *Ptf1a*, promoting the differentiation of glycinergic and GABAergic AC, where their concurrent knockdown has an opposing effect (Jin *et al.*, 2015). This study defined a *Foxn4-Ptf1a-Tcfap2a/Tcfap2b* genetic cascade that defines the differentiation of amacrine and horizontal cells during retinogenesis (Jin *et al.*, 2015). However, previous work from our laboratory, and from this thesis, contrast with these studies with evidence suggesting that AP-2 $\alpha$  and AP-2 $\beta$  are not required for the generation of AC (Bassett *et*

*al.*, 2007; 2010; 2012). Changes in the migration and lamination of AC was affected in the double conditional mice but the number of cells did not appear to significantly diminish upon loss of AP-2 $\alpha$  and AP-2 $\beta$  (Bassett *et al.*, 2012; Zaveri, 2014). Further research into the major glycinergic and GABAergic, as well as the subset of cholinergic AC populations in adult mice are further addressed in this thesis.

### **1.2.2. Mosaic Patterning of Amacrine Cells**

Retinal mosaic patterning is not well understood, particularly the arrangement of AC in the INL and GCL. All neurons establish specific pattern of distribution of soma to minimize distance between homotypic cells with dendrites distributed evenly over the surface. Upon differentiation, neurons migrate to their final positions and respond to environmental cues for organizing cell bodies in a non-random pattern. Regular retinal mosaics allow visual images to be processed uniformly across many neurons. The AC mosaic is particularly important for extracting visual data related to direction of motion of the ON and OFF visual pathways (Whitney *et al.*, 2008). The correct movement and position of post-mitotic retinal neurons has been the subject of many studies (Galli-Resta *et al.*, 2008). Studies in mice have demonstrated that certain retinal neurons can migrate tangentially over a short distance to a final position (Reese & Galli-Resta, 2002). This lateral movement is characteristic of cone PRs, HC, AC and GCs, and is one of several mechanisms responsible for the regular spacing of like cells, or mosaic formation, that is central to retinal organization (Galli-Resta *et al.*, 2008). As AC move basally, they appear to assess their environment through random, dynamic process outgrowth (Godinho *et al.*, 2005). When developing neurons reach their final laminar position, mosaics are thought



to be formed through interactions with surrounding homotypic cells, and are assembled independently of other cell types (Galli-Resta *et al.*, 2008).

Retinal mosaics typically follow a “minimal spacing rule” in which a certain distance must be maintained between homotypic cells (Reese & Galli-Resta, 2002). Repulsive interactions mediated by semaphorins and their receptors, plexins, regulate dendritic self-avoidance in the retina (Matsuoka *et al.*, 2012). In semaphorin KO mice, cells develop asymmetric arbors with abundant self-crossovers (Sun *et al.*, 2013). A cadherin-like transmembrane protein, protocadherin, has been shown to shape the branching pattern in a variety of AC subtypes. (Lefebvre *et al.*, 2008). In its absence, cells develop asymmetric morphology, often fasciculating with their own dendrites (Lefebvre *et al.*, 2012). DSCAM prevents cell-to-cell interactions that mediate adhesion, allowing dendrites to freely extend amongst homotypic dendrites (Keeley *et al.*, 2012). Absence of DSCAM resulted in the clustering of somas of melanopsin-positive GCs and dopaminergic ACs and fasciculations of retinal processes (Fuerst *et al.*, 2008; 2009). DSCAM and other cell adhesion molecules, such as protocadherin, are regulated by a variety of transcription factors. For example, Pax6 controls the expression of cadherin family members, such as neural adhesion molecule L1 (Chalepakis *et al.*, 1994). Interestingly, AP-2 $\alpha$  regulates the expression of E-cadherin (Beherens *et al.*, 1992; Pontoriero *et al.*, 2008). Regulation of cell adhesion molecules remains largely unknown. The discovery of these regulatory factors would give insight into the developmental controls involved in mosaic patterning. This would allow not only the understanding of pathways to neural commitment for a specific fate, but also identify genes required to

dictate synaptic interactions to understand complex networks of retinal connectivity further.

### **1.2.3 Electrophysiology of the Eye**

The correct patterning and positioning of cells in the retina is important for proper transduction of electrical signals. The absorption of light by visual pigments in the outer segments of PRs triggers the transduction of light into a neuronal signal passed to the brain *via* GC axons of the optic nerve. There are several neuronal processes that transform the simple point absorption of the PR signal to the receptive field of the GCs. Interneurons in the inner layers of the retina refine the signals and process them such that information about contrast and intensity are given to the GC (Kolb, 2003). Vertical integration occurs between the PRs and GC by the connection provided by BC while the HC and AC process information orthogonally to the BC (Wässle, 2004). The GC receptive field is therefore made up of information derived from the integration of many PR cells by the interneurons (Hoon *et al.*, 2014).

The light-induced changes in the membrane potential of retinal cells can be detected by an electroretinogram (ERG) as currents that flow within the eye in response to light can be analyzed into component ‘waves’ resulting from specific sets of cells (Pinto *et al.*, 2007). Despite extensive research on the cellular origins of the ERG recordings, the precise mechanisms are still unclear. The PRs are the source of the negative going a-wave, it is the cessation of a standing photocurrent that flows constantly in the dark (Pinto *et al.*, 2007). The ERG b-wave has been a topic of debate because it is the major

component of the human ERG recordings used in clinical and experimental analysis of retinal function. The b-wave originates in the retinal cells post-synaptic to the PRs and blocking synaptic transmission from the PR to second order retinal neurons eliminates the ERG b-wave (Nir *et al.*, 2002). It was once thought the b-wave mainly reflects light-induced activity of ON BC and MG (Tian & Slaughter, 1995). Other neurons may modulate the b-wave under certain conditions and both OFF BC and HC have been shown to affect the amplitude and kinetics of the b-wave (Sieving *et al.*, 1994). Third-order neurons are now known to make a significant contribution to the amplitude of the b-wave after pharmacological manipulation of these neurons altered the amplitude of the b-wave (Dong & Hare, 2000). It has also been proposed that GABA feedback from AC to BC can affect the b-wave. Blocking this feedback has a profound impact on the b-wave amplitude and demonstrates the impact of AC in b-wave generation (Dong & Hare, 2002).

### **1.3 Activating Protein-2**

Studies from our lab have shown the AP-2 family of transcription factors are important regulators of eye development. AP-2 $\alpha$  is known to play a role in lens morphology (West-Mays *et al.*, 1999; Pontoriero *et al.*, 2008), OC patterning (Bassett *et al.*, 2007), and retinogenesis (Bassett *et al.*, 2010; 2012). The AP-2 family consists of five different transcription factors, AP-2 $\alpha$ - $\epsilon$ , which form homo- and heterodimers. AP-2 proteins expressed in humans and mice are encoded by separate genes exhibiting overlapping and unique expression profiles in derivatives of the neural crest and surface ectoderm, renal and urogenital tissues, limb buds, and structures of the CNS including the

retina (Mosher *et al.*, 1997, Hilger-Eversheim *et al.*, 2000). The AP-2 proteins bind to target sequences by a basic DNA-binding domain, coded by exons 4-7, that binds to a palindromic consensus sequence, followed by a characteristic helix-span-helix motif facilitating dimerization and DNA binding (Fig. 5) (Eckert *et al.*, 2005).

AP-2 $\alpha$  is expressed in numerous tissues throughout embryonic development including the lens and retina (Hilger-Eversheim *et al.*, 2000). Germ-line deletion of AP-2 $\alpha$  exhibits severe developmental defects due to death of migrating neural crest cells resulting in the cranial neural tube and abdomen failing to close (Hilger-Eversheim *et al.*, 2000). Our lab has shown the germline AP-2 $\alpha$  KO mice exhibit ocular defects, abnormal lens, cornea, RPE and NR (West-Mays *et al.*, 1999). Due to the severity of developmental defects, these AP-2 $\alpha$ <sup>-/-</sup> mice die prenatally and ocular development cannot be examined past birth (Hilger-Eversheim *et al.*, 2000). To determine if AP-2 $\alpha$  has a cell-autonomous role in the developing retina, our lab conditionally deleted AP-2 $\alpha$  from the presumptive retina with Cre-loxP technology (Bassett *et al.*, 2007). No detectable abnormalities were observed and thus compensatory role of another family member with similar expression, AP-2 $\beta$ , was proposed (Bassett *et al.*, 2007). The redundant, compensatory role of these two family members was further exemplified in that AP-2 $\beta$  germ line KO mice had normal cranial structures and neural tissues even though these normally express high levels of AP-2 $\beta$  (Moser *et al.*, 1997).

The increase of AP-2 $\beta$  expression in AP-2 $\alpha$  deleted regions suggested AP-2 $\beta$  may compensate for the loss of AP-2 $\alpha$  (Bassett *et al.*, 2010). AP-2 $\alpha$  and AP-2 $\beta$  have similar embryonic expression patterns and have been suggested to share a common ancestor due

to the high degree of conservation in their structure and protein sequence (Moser *et al.*, 1995). Sharing 92% similarity in the dimerization and DNA binding regions, AP-2 $\alpha$  and AP-2 $\beta$  bind to each other *in vitro* and to identical sites on a given promoter to regulate the transcription of the same genes (Zhu *et al.*, 2001). This led to a mutant model in which the conditional AP-2 $\alpha$  mutants were crossed with AP-2 $\beta$  germ-line KO mice (Bassett *et al.*, 2012). As the double KO mutants do not survive past birth, due to germ-line deletion of AP-2 $\beta$  the study of retinogenesis is limited to embryonic stages. To circumvent this problem, our lab has acquired the AP-2 $\beta$  “floxed” mouse line, allowing for selective deletion of AP-2 $\beta$  from the retina. AP-2 $\beta$  “floxed” mice were bred with the AP-2 $\alpha$  “floxed” line to generate a homozygous floxed line for AP-2 $\alpha$  and AP-2 $\beta$ . These mice were incorporated into the breeding scheme outlined in Figure 6 and the double conditional KOs produced only displayed defects in the peripheral retina (where the Pax6  $\alpha$ -cre promoter is active). This double conditional approach enables the mice to survive well into adulthood and facilitates the studies in this thesis of the AP-2 genes in postnatal retinogenesis.

Preliminary data from our lab has shown a complete loss of HC in post-natal double mutants in the regions where AP-2 $\alpha$  and AP-2 $\beta$  were conditionally deleted (Zaveri, 2014). In addition, structural changes in the OPL, absence of triad ribbon synapses of rod PR, defects in the PR axons, and abnormal cellular lamination was observed. Double knockout mice showed a striking loss of horizontal cells however, amacrine cell populations appeared to be maintained. The adult retina expresses AP-2 $\alpha$  and AP-2 $\beta$  in the glycinergic and GABAergic populations, with GABAergic expressing AC found as

early as E14.5 while the glycinergic AC population peaks at P0 (Bassett *et al.*, 2012). Cholinergic AC are one of the earliest subsets of GABAergic AC found in the retina and in the embryonic double KO studies, these cells exhibit irregular cell arrangement compared to controls (Bassett *et al.*, 2012). These mice could not be examined past-birth due to the lethality of germ-line deletion of AP-2 $\beta$ . Retinogenesis continues to P14, therefore it is imperative to examine the effect the loss of AP-2 $\alpha$  and AP-2 $\beta$  may have on AC and this will be the focus of my thesis.

## **CHAPTER TWO**

### **Rationale, Main Hypothesis & Research Aims**

## 2.1 Rationale for Study

The eye is an ideal model providing insight into the complex intricacies of fundamental biological processes including morphogenesis, pattern formation, cell fate determination and differentiation. Due to its peripheral location, the eye can be manipulated and studied from embryogenesis into adulthood, facilitating the understanding of the genetic code underlying development. In particular the retina, as an extension of the central nervous system, can give insight into the complexities of neurogenesis.

Many genes govern the development of the neurons and glia in the retina and their correct cellular arrangement. Investigation into the role of the transcription factor family Activating protein-2 in eye development has been the focus of our lab for a number of years. The purpose of this project is to further understand the roles of AP-2 in the developing and adult mouse retina by elucidating the downstream effects following deletion of AP-2 $\alpha$  and AP-2 $\beta$  in the retina during embryogenesis.

Previous data from our lab has shown AP-2 $\alpha$  and AP-2 $\beta$  as the major AP-2 family members expressed in the HC and AC lineage of the retina, and they have overlapping roles in the development of both cell types (Bassett *et al.*, 2007; 2010; 2012). In mice lacking both AP-2 $\alpha$  and AP-2 $\beta$ , a complete loss of HC was observed at birth and this was accompanied by the failure of AC to achieve correct laminar positioning and homotypic spacing (Bassett *et al.*, 2012). However, due to germ-line deletion of AP-2 $\beta$  in these



mice, they did not survive long after birth, and retinogenesis could not be examined to completion.

Given the overlapping expression of AP-2 $\alpha$  and AP-2 $\beta$  in post-mitotic AC and earlier work demonstrating that the deletion of these two genes may disrupt AC displacement, further investigation of the double conditional mutant mice is necessary during post-natal stages when retinogenesis is complete. In the following thesis, I will further elucidate the role(s) of AP-2 $\alpha$  and AP-2 $\beta$  in AC mosaic patterning and determine how alteration in patterning may have downstream effects of the physiological function of the retina.

## **2.2 Main Hypothesis**

**The conditional deletion of both AP-2 $\alpha$  and AP-2 $\beta$  from the developing retina will result in irregular cholinergic amacrine cell mosaic patterning and defects in retinal electrophysiology, which is not observed upon single deletion of either gene.**

## **2.3 Specific Aims**

*2.3.1 Examine and analyze the amacrine cell mosaic patterning in conditional knockout mice.*

Using the breeding schemes described in Figures 6 and 7, double and single conditional knockout mice were made using Cre-loxP technology. Amacrine cells in the inner nuclear layer and ganglion cell layer are vital for both ON and OFF visual pathways

as they participate in the extraction of the direction of motion with their mosaic fundamental for proper visual processing (Whitney *et al.*, 2008). Voronoi domain and nearest-neighbour analyses will be used to compare the regularity of cholinergic amacrine cell mosaics in the single and double conditional knockouts and compared to those of control littermates.

*2.3.2. Examine and analyze retinal function in conditional knockout mice.*

Previous work from our lab has shown a complete loss of horizontal cells and changes in the photoreceptors and their synaptic connections. Correct visual processing depends on regular patterning and composition of all retinal cells. The loss of HC and PR synapse alteration, along with the irregularities seen in cholinergic amacrine cell mosaics in the double conditional knockout mice may result in functional abnormalities in retinal physiology when compared with control and single knockout models. The function of the conditional knockout mouse retinas will be determined *in vivo* using full-field, scopic electroretinograms.

*2.3.3. Examine the genetic cascades in retinal amacrine cell development.*

There is a complex hierarchy of factors involved in horizontal and amacrine cell development. This aim will further elucidate the role of the AP-2 $\alpha$  and AP-2 $\beta$  in retinal development. Downstream amacrine markers will be used in the double conditional mutants to determine if their expression is disrupted, indicating that these AP-2 genes are involved in the transcriptional regulation of these neurons.

**CHAPTER THREE**  
**Experimental Design**

### 3.1 Generation of Mouse Lines

All animal procedures were performed in accordance with the Association for Research in Vision and Ophthalmology (ARVO) Statement for the Use of Animals in Ophthalmic and Vision Research. The series of crosses used to generate conditional *Tcfap2a/Tcfap2b* knockout mutants (DBL KO) is depicted in Figure 6 with all crosses on a C57BL/6 background. Two *Tcfap2* alleles were incorporated into the breeding scheme. These alleles include the *Tcfap2a*<sup>ki7lacZ</sup> null allele [due to germ-line IRES-lacZ knock-in insertion disrupting exon 7] (Brewer *et al.*, 2002); and a *Tcfap2b*<sup>KO</sup> null allele [due to the germ-line insertion of a PGK-neo cassette disrupting exon 4] (Moser *et al.*, 1997).

*Tcfap2a*<sup>ki7lacZ/+</sup> mice were crossed with  $\alpha$ -Cre<sup>+/-</sup> transgenic mice (Marquardt *et al.*, 2001) expressing Cre recombinase under control of the retina-specific ‘Pax6  $\alpha$  enhancer’ from the murine Pax6 gene.  $\alpha$ -Cre<sup>+/-</sup>/*Tcfap2a*<sup>ki7lacZ/+</sup> mice were then crossed with *Tcfap2b*<sup>+/-</sup> mice to generate mice that had only one functional copy of *Tcfap2a* and *Tcfap2b*, and retained the expression of the  $\alpha$ -Cre transgene.

In a second cross, homozygous *Tcfap2a*<sup>lox/lox</sup> mice (Brewer *et al.*, 2004) were bred with mice homozygous for the *Tcfap2b*<sup>lox/lox</sup> allele (Green, unpublished) in which exons 5 and 6 of *Tcfap2a* and exon 6 of *Tcfap2b* are flanked by single loxP sites to obtain *Tcfap2a*<sup>lox/lox</sup>/*Tcfap2b*<sup>lox/lox</sup> mice that were homozygous floxed for both alleles. This allows for the second copy of *Tcfap2a* and *Tcfap2b* to be conditionally deleted by Cre-mediated excision (Fig. 8). The final cross of this breeding scheme is expected to result in

only one-eighth of the offspring being conditional double mutants, therefore many breeders are required.

The same *Tcfap2* alleles and Cre-recombinase were used to create single conditional mutants as described in Figure 7. In these mating pairs, only one AP-2 family member was deleted, either *Tcfap2a* ( $\alpha$ KI) or *Tcfap2b* ( $\beta$ KO), while the other *Tcfap2* alleles remained unaltered. For example,  $\alpha$ -Cre<sup>+/-</sup> transgenic mice were bred with *Tcfap2a*<sup>ki7lacZ/+</sup> and the resulting offspring,  $\alpha$ -Cre<sup>+/-</sup>/*Tcfap2a*<sup>ki7lacZ/+</sup> were crossed with homozygous floxed *Tcfap2a*<sup>lox/lox</sup> mice. This breeding scheme allows for the conditional KO of only *Tcfap2a* from the retina, while *Tcfap2b* remains the same ( $\alpha$ -Cre<sup>+/-</sup>/*Tcfap2a*<sup>ki7lacZ/lox</sup>).

For all genotyping, DNA was extracted from adult ear clips using the EZNA Tissue DNA Kit (Omega Bio-Tek). Genotypes were determined by previously established polymerase chain reaction (PCR) protocols (Table 1). Littermates used as controls either contained two functional copies of *Tcfap2a* and *Tcfap2b* in the retina, or were missing one functional copy of either allele if the former was not available.

### **3.2 Histology**

Dissected whole eyes were collected from KO mice and control littermates euthanized by CO<sub>2</sub> overdose. Tissue was fixed in 10% neutral buffered formalin (Sigma-Aldrich, Oakville, ON) for 24 hours then stored in 70% ethanol. Samples were processed (Core Histology Lab, McMaster University) and embedded in paraffin (Paraplast Tissue

Embedding Media, Fischer Scientific, Waltham, MA). Serial sections were cut to 4  $\mu\text{m}$  in thickness and used for immunofluorescent analysis.

### **3.3 Immunofluorescence**

Indirect immunofluorescence was performed on paraffin sections using the primary antibodies listed in Table 2. Sections were deparaffinised in xylene, hydrated (through 100%, 95% 75% ethanol, followed by water), treated with 10mM sodium citrate buffer (pH 6.0; boiling for 20 minutes) for antigen retrieval, blocked with normal goat or donkey serum, and incubated with primary antibodies overnight at 4°C. Fluorescent secondary antibodies Alexa Fluor 568 nm or 488 nm (Invitrogen/Molecular Probes, Burlington, ON) were used 1:200 for 1 hour at room temperature. For all colocalization studies, both primaries and both secondaries were mixed and incubated simultaneously. All stains were mounted with ProLongGold antifade mounting medium with 4,6-diamino-2-phenylindole (DAPI; Vector Laboratories, Burlington, ON).

All stains were visualized with a microscope (Leica, Deerfield, IL) equipped with an immunofluorescent attachment, and images were captured with a high-resolution camera and associated software (Leica Application Suite X; LasX). Images were reproduced for publication with image management software (Photoshop CC 2017, Adobe Systems Inc., Mountain View, CA).

### **3.4 Cell Counting Studies**

To quantify amacrine cells in the different knock out strains, immuno-labelled cells in a 600  $\mu\text{m}$  length of retinal section equidistant from the periphery were counted in

a minimum of three sections from three different animals and expressed as the mean  $\pm$  standard deviation (SD). Data were tested for significance by one-way ANOVA (GraphPad Prism 7) comparing the different conditional knockout groups to a common control. Bonferroni post-hoc comparisons were made when statistical significance ( $P < 0.05$ ) was found between observations. A samples size of 3 knockout and 3 control retinas minimum were used for each strain. Sections closely preceding or following those used for cell counts were previously stained with anti-AP-2 $\alpha$  or anti-AP-2 $\beta$  to confirm deletion in these regions.

### **3.5 Flat Mount Retinas**

Mouse eyes were removed and fixed for 2 hours in 4% buffered formalin. Retinas were dissected whole, rinsed in PBS, and permeabilized overnight with 0.3% Triton X-100 in PBS (PBST). Retinas were then blocked in normal serum for three hours at room temperature and transferred to a primary antibody solution containing 1% DMSO and 5% normal serum in PBST and agitated for 72 hours at 4°C. Retinas were subsequently washed in PBST and incubated in Alexa Fluor secondary antibodies (1:200) in PBST with 1% DMSO and 2.5% normal serum for 4 hours at room temperature. Retinas were lastly rinsed in PBS before being flat mounted on clean slides with ProLongGold antifade mounting medium with DAPI.

Flat mount retinas were examined using a 20x objective on a Leica microscope equipped for fluorescence using the associated camera and computer software. Fields were sampled from the peripheral retina, approximately two-thirds from the optic nerve

head, in four quadrants, sampling cholinergic amacrine cell mosaics in both the INL and GCL in the eight loci. For each field, Voronoi domain (VD) and nearest-neighbour (NN) values were calculated using FIJI software with associated plug-ins (NIH). Threshold values were set for each fluorescent image to isolate immuno-positive cells of interest. The image was then converted to binary and the Voronoi domain plug-in was utilized. Areas for each bound cell were calculated. The VD area is the area of all points in the plane of the retina closer to that one cell than to any other cells while the nearest neighbour distances measure how close homotypic cells are in relation to one another. The collection of NN distances and VD areas were then used to calculate a regulatory index (RI), being the average NN or VD divided by its standard deviation. Comparisons were tested for significance with one-way ANOVA (GraphPad Prism 7). Bonferroni post-hoc comparisons were made when statistical significance ( $P < 0.05$ ) was found between observations. For each group, 4 retinas were analysed with all values expressed as the mean  $\pm$  SD.

### **3.6 Electroretinograms**

Scopic full-field ERGs (Ganzfeld ERG; Phoenix Research Laboratories, Pleasanton, CA, USA) were recorded from dark-adapted mice (12 hours) under dim, red light (750 nm). Animals were anesthetized with 2.5% avertin (0.015 ml/mg B.W) intraperitoneally, supplemented as necessary subcutaneously. Pupils were dilated with 0.5% Tropicamide and 2.5% Phenylephrine Hydrochloride Ophthalmic Solutions (AKORN, Lake Forest, IL). Tear-Gel ophthalmic liquid gel (Alcon Canada, Mississauga,



ON, Canada) was applied throughout the procedure to prevent drying of the cornea and to maintain coupling of the corneal electrode.

Animals were placed on a heated platform (37°C) with a platinum plated ground electrode placed in the base of the tail and a platinum reference electrode placed in the scalp, between the ears. The gold-plated corneal electrode was positioned in contact with the Tear-Gel solution on the cornea, completing the circuit. Series of 2 ms, single-flash recordings were obtained using a LED stimulus (504 nm) at increasing light intensities (-1.6 to 3.0 log cd\*s\*m<sup>-1</sup>) with 20 responses recorded for low level stimuli, to 3 for the highest flash intensities. The inter-stimulus interval increased from 1 second for low stimuli to 120 seconds for the highest. The a- and b-wave amplitudes of the resulting ERGs were evaluated using associated software (LabScribe; iWork System Inc., Dover, NH). 3 eyes were examined for each group expressed as the mean ± SD. A two-way repeated ANOVA was performed to analyze the effects of genotype and the repeated light intensity measures on a- and b-wave amplitudes. Post-hoc analysis using Tukey's HSD indicated at which light intensities the amplitudes were different between genotypes. Statistical significance defined as P<0.05.

**Table 1.** PCR Protocols for Genotyping.

<b>Alleles</b>	<b>Primers</b>	<b>Conditions</b>	<b>Products</b>
AP-2 $\alpha^{ki7lacZ}$ vs AP-2 $\alpha^{+/+}$	<b>Alpha 3'KO</b> 5'-CGT GTG GCT GTT GGG GTT GTT GCT GAG GTA C-3' <b>Alpha 6/7</b> 5'-GAA AGG TGT AGG CAG AAG TTT GTC AGG GC-3' <b>IRESUP</b> 5'-GCT AGA CTA GTC TAG CTA GAG CGG CCC GGG-3'	45 s at 95°C, 1 min at 67°C, 1 min 10 s at 72°C for 33 cycles	<i>Tcfap2a<sup>ki7lacZ</sup></i> 300 bp  <i>Tcfap2a<sup>+</sup></i> 500 bp
AP-2 $\alpha^{lox}$ vs AP-2 $\alpha^{+}$	<b>Alflox4</b> 5'-CCC AAA GTG CCT GGG CTG AAT TGA C-3' <b>Alfscsq</b> 5'-GAA TCT AGC TTG GAG GCT TAT GTC-3'	45 s at 95°C, 45 s at 65°C, 1 min at 72°C for 39 cycles	<i>Tcfap2a<sup>lox</sup></i> 560 bp  <i>Tcfap2a<sup>+</sup></i> 490 bp
AP-2 $\beta^{+/+}$ vs AP-2 $\beta^{+/+}$	<b>4 Exon DW</b> 5'-CCT CCC AAA TCT GTG ACT TCT-3' <b>PGK-PolyA</b> 5'-CTG CTC TTT ACT GAA GGC TCT TT-3' <b>4 Exon Rev</b> 5'-TTC TGA GGA CGC CGC CCA GG-3'	45 s at 95°C, 45 s at 58°C, 1 min at 72°C for 37 cycles	<i>Tcfap2b<sup>-</sup></i> 380 bp  <i>Tcfap2b<sup>+</sup></i> 221 bp
AP-2 $\beta^{lox}$ vs AP-2 $\beta^{+/+}$	<b>BFL8</b> 5'-GTC TGT TTA GAA CCT GGC TCA GCC AG-3' <b>BFL9</b> 5'-TCT GGC AAG GCT CTT TCG GGG CAC TC-3' <b>BFL10</b> 5'-CGC AGC GCA TCG CCT TCT ATC GCC TT-3'	2 min at 95°C, 45 s at 95°C, 3 min at 70°C for 34 cycles	<i>Tcfap2b<sup>lox</sup></i> 550 bp  <i>Tcfap2b<sup>+</sup></i> 450 bp
$\alpha$ -Cre	<b>Cre1</b> 5'-GCT GGT TAG CAG CGC AGG TGT AGA G-3' <b>Cre3</b> 5'-CGC CAT CTT CCA GCA GGC GCA CC-3'	45 s at 95°C, 1 min at 67°C, 1 min 10 sec at 72°C for 33 cycles	Presence of $\alpha$ - <i>Cre</i> transgene 420 bp

**Table 2.** List of Antibodies for Immunofluorescence.

<b>Antibody</b>	<b>Supplier</b>	<b>Working Concentration</b>
Mouse anti-AP-2 $\alpha$	3B5; Developmental Studies Hybridoma Bank, University of Iowa, Iowa City, IA	1:1 (sections) 1:100 (flat mounts)
Rabbit anti-AP-2 $\beta$	#2509; Cell Signaling Technology, Danvers, MA	1:50
Goat anti- $\beta$ 3 (BHLHB5)	E-17 #sc-6045; Santa Cruz Biotechnology, Santa Cruz, CA	1:400
Mouse anti-Calbindin	Clone CL-300, Product #C8666; Sigma-Aldrich, Oakville, ON	1:250
Goat anti-Calretinin	N-18 #sc-11644; Santa Cruz Biotechnology, Santa Cruz, CA	1:800
Goat anti-ChAT	AB144P; EMD Millipore, Billerica, MA	1:100
Goat anti-Glyt1	AB1770; Millipore-Chemicon, Billerica, MA	1:5000
Rabbit anti-GAT1	Ab426; Abcam, Cambridge, MA	1:250
Rabbit anti-Sox2	AB5603; Millipore-Chemicon, Billerica, MA	1:800
<b>Secondary:</b>		
Alexa Fluor 568	Invitrogen – Molecular Probes, Burlington, ON	1:200
Alexa Fluor 488	Invitrogen – Molecular Probes, Burlington, ON	1:200

## **CHAPTER FOUR**

### **Results**

#### 4.1 Generation of *Tcfap2a*, *Tcfap2b*, and *Tcfap2a/b* Conditional KO Mice

Mice with homozygous global deletion of *Tcfap2a* or *Tcfap2b* are not viable or die shortly after birth. Conditional deletion of *Tcfap2a*, *Tcfap2b*, or both, from the developing retina was achieved through use of the breeding schemes outline in Figures 6 and 7. Five mouse lines were used to create  $\alpha$ KI (*Tcfap2a*<sup>ki7lacZ/lox</sup>),  $\beta$ KO (*Tcfap2b*<sup>KO/lox</sup>), or DBL (*Tcfap2a*<sup>ki7lacZ/lox</sup>/*Tcfap2b*<sup>KO/lox</sup>) KOs. The breeding scheme utilized *Tcfap2a* and *Tcfap2b* heterozygotes so that Cre-loxP-mediated excision was only required for only one of each allele (Fig. 8). *Tcfap2* heterozygotes are incorporated into the crosses instead of utilizing only the *Tcfap2a*<sup>lox/lox</sup> or *Tcfap2b*<sup>lox/lox</sup> homozygotes to ensure there is no dilution of the Cre-recombinase efficiency. Mice from the final crosses were genotyped from using DNA extracted from ear clips. The different AP-2 alleles  $\alpha$ KI lacZ,  $\alpha$ flox,  $\beta$ het,  $\beta$ flox, and presence of Cre recombinase were detected through PCR analysis. Once a sample was positive for all fragments necessary for the single AP-2 $\alpha$  and AP-2 $\beta$  deletion, or both, the mice were used for *in vivo* dark-adapted electroretinograms followed by immunofluorescence of the whole retina, or their eyes were processed and the expression of AP-2 $\alpha$  and AP-2 $\beta$  was examined in histological sections.

The Cre recombinase is under control of the *Pax6*  $\alpha$  enhancer, which is a retina-specific regulatory element of the mouse *Pax6* gene (Marquardt *et al.*, 2001) activated at E10.5. When activated, this Cre-mediated excision leads to the loss of AP-2 $\alpha$  and AP-2 $\beta$  expression in the peripheral retina. Adult mice, 2 months of age, were used for all analyses as previous work has extensively examined AP-2 $\alpha$  and AP-2 $\beta$  expression in the developing retina (Bassett *et al.*, 2007; 2010; 2012). To ensure deletion was successful

from the neural retina, AP-2 $\alpha$  and AP-2 $\beta$  expression was monitored *via* immunofluorescence in  $\alpha$ KI,  $\beta$ KO, and DBL KO mutants and compared to littermate controls (Fig. 9). AP-2 $\alpha$  and AP-2 $\beta$  expression was readily detected in the INL and GCL in the periphery of control retinas, with a clear deletion observed in those regions of the DBL KOs. Single  $\alpha$ KI mice demonstrated a loss of AP-2 $\alpha$  expression while AP-2 $\beta$  expression remained comparable to that of the control. Similar results were seen in  $\beta$ KO mutants with AP-2 $\alpha$  expression remaining unchanged while AP-2 $\beta$  was no longer readily visible.

#### **4.2 Cholinergic Amacrine Cell Mosaics are Altered by Deletion of AP-2 $\alpha$ and AP-2 $\beta$ from the Retina**

Visual processing relies on the correct arrangement of neurons within the retina. Amacrine cells in the INL and GCL are vital for both ON and OFF visual pathways, as they participate in the extraction of the direction of motion with their mosaic fundamental for proper visual processing (Whitney *et al.*, 2008). Currently, the preferred method for examining the regularity of retinal mosaics is measuring the Voronoi domain (VD) areas and nearest-neighbour (NN) distances in flat mount retinas (Whitney *et al.*, 2008). The VD of a cell is the area of all points in the plane of the retina that are closer to that cell than to any other cell measuring the regularity in the coverage of the retina by these cells while the NN distances determine the proximity of the homotypic cells (Fig. 10). Whole retinas were immunolabelled with ChAT and AP-2 $\alpha$  or AP-2 $\beta$ , with samples taken from the periphery, approximately two-thirds from the optic nerve head, in both the INL and GCL in each of the four quadrants with the NN distances and VD areas calculated for all ChAT-positive cells (Fig. 11; Fig 13). The collection of NN distances and VD areas were

then divided by their respective standard deviations to calculate a regularity index (RI), with a regular arrangement and patterning of cells exhibiting a small standard deviation around the mean, causing the RI value to increase. The mosaics of cholinergic AC in the INL appear more regular than the mosaics within the GCL, regardless of the mouse strain examined. For example, the nearest neighbour regularity index (NNRI) confirmed this difference between the layers in every strain with an average NNRI of  $3.74 \pm 0.43$  for the INL samples, while the GCL was significantly lower,  $2.74 \pm 0.25$ ,  $P < 0.011$ . The average VDRI, while not significantly different ( $P < 0.15$ ), followed a similar trend with a greater regularity index seen in the INL,  $2.60 \pm 0.61$ , than that for the GCL,  $2.02 \pm 0.28$ .

Examination of the effect of deletion of AP-2 $\alpha$ , AP-2 $\beta$  or AP-2 $\alpha$  and AP-2 $\beta$  from the retina on the NNRI showed a significant decrease in INL of double KO mice when compared with controls (Fig. 12), while neither  $\alpha$ KI nor  $\beta$ KO retinas displayed a significant difference in NNRI values compared to control littermates. The decrease in NNRI values was significant in the INL with an average double KO NNRI of  $3.12 \pm 0.60$  compared to  $4.19 \pm 0.39$  in the INL of controls ( $P < 0.03$ ). No significant difference was observed between the VDRI of any mutant strain and the control in the GCL (Fig. 14). However, the VDRI significantly decreased in the INL of double KO mice when compared to controls, falling to  $1.75 \pm 0.38$  from  $3.38 \pm 0.68$  ( $P < 0.01$ ). These values suggest that these AP-2 transcription factors are required for ensuring the proper spacing of cholinergic amacrine cells.

The cholinergic amacrine cells are one of the earliest born subtypes of the GABAergic population, forming a regular patterned distribution in the late embryonic

retina (Galli-Resta *et al.*, 1997). In an earlier study, histological sections of embryonic DBL KO eyes revealed that while the amacrine cell population numbers were not significantly affected after the deletion of AP-2 $\alpha$  and AP-2 $\beta$ , their distribution in the INL and GCL was disorganized when compared to controls (Bassett *et al.*, 2010). Histological sections limit our ability to accurately determine how the spacing of AC mosaics may be affected. Thus, to more assess cholinergic AC patterning in the post-natal single and double conditional KO mice, immunofluorescence analyses of whole retinas were performed using a cholinergic AC-specific marker, choline acetyltransferase (ChAT) along with AP-2 $\alpha$  or AP-2 $\beta$ . In tissue sections, there was no significant change observed in the number of ChAT labelled AC, however it was difficult to ascertain how the spatial arrangement of ChAT labelled AC in  $\alpha$ KI,  $\beta$ KO or the double KO mice retinas may differ from controls (Fig. 15). However, looking at the retina as a whole within the flat mount studies, it is clear that ChAT-positive cell populations have altered patterning in the knockout models observed, highlighting the advantage of flat mount mosaic patterning studies.

#### **4.3 The Physiological Response to Light is Altered by Loss of AP-2 $\alpha$ and AP-2 $\beta$ from the Retina**

As previously stated, correct visual processing depends on the proper arrangement and functionality of all retinal neurons. Previous work from our lab has shown a complete loss of HCs and irregularities in AC positioning (Bassett *et al.*, 2012) as well as changes in the PRs and their synaptic connections in retinas where both AP-2 $\alpha$ /AP-2 $\beta$  were deleted (Zaveri, 2014). Proper PR synapse development is necessary to transduce visual stimuli to the HC and AC of the inner retina where the signals are further modulated, with



disruption in this signal cascade causing changes in the functional response of the retina (Dick *et al.*, 2003; Elgueta *et al.*, 2015; Sonntag *et al.*, 2012). To determine the effect these changes, dark-adapted full field ERGs were used to compare  $\alpha$ KI,  $\beta$ KO, and double KOs with control littermates. Moreover, the ERGs measure the impact of irregular AC mosaic patterning on the function of the retina. Control mice retinas were found to exhibit typical ERG waveforms characteristic of dark adapted mice with a negative a-wave, depicting the hyperpolarization of rod PRs, and a positive b-wave representative of the depolarization of interneurons including HC, BC, and AC (Fig. 16). As light intensity was increased, the response in control retinas also increased with larger negative a-wave amplitudes and positive b-wave amplitudes observed. Comparatively, double KO mice showed a similar a-wave response with the amplitude negatively increasing with brighter flashes of light that was not consistently different from the control at the flash intensities measured, with an occasional significant difference occurring most likely due to inter-strain variability ) (Fig. 17). However the b-wave response deviated from that seen in controls (Fig. 18). As light intensity was increased, the b-wave amplitude began to increase until a flash intensity of  $-1.108 \log \text{cd} \cdot \text{s} \cdot \text{m}^{-2}$ , where it significantly differed from controls ( $P < 0.0003$ ) and continued to significantly diverge from controls at all increasing flash intensities as the b-wave amplitude appeared to plateau ( $P < 0.0001$ ) (Fig. 18).

Single conditional knockouts,  $\alpha$ KI and  $\beta$ KO demonstrated similar a-wave responses to those seen in control mice, with larger negative values seen for higher flash intensities and no significant difference recorded ( $P > 0.05$ ) (Fig.17). When AP-2 $\alpha$  is deleted from the retina and AP-2 $\beta$  expression remains intact, as seen in  $\alpha$ KI mutants, the

b-wave amplitudes exhibit a similar trend to seen in controls, increasing with light intensity. Interestingly, when AP-2 $\beta$  is deleted from the retina, b-wave amplitudes have a decreased response to light intensity compare to controls, while AP-2 $\alpha$  expression remains unchanged (Fig. 18). The b-wave amplitude begins to deviate from controls at a flash intensity of 0.875 log cd\*s\*m<sup>-2</sup> and continues to be significantly different at increasing light intensities (P<0.0001). Unlike the double KO mice where b-wave amplitudes appear to peak after a certain level of light intensity, the b-wave amplitudes in  $\beta$ KO mice continue to increase but not to the same extent as controls or  $\alpha$ KI mice. These findings suggest that downstream effects of deleting AP-2 $\alpha$  and AP-2 $\beta$  from the retina may decrease the physiologic response to light, and that AP-2 $\beta$  may be more significant in this process than AP-2 $\alpha$ .

#### **4.4 Amacrine Cell Development is not Dependent on AP-2 $\alpha$ and AP-2 $\beta$**

The majority of amacrine cells in the mammalian retina contain either glycine or  $\gamma$ -Aminobutyric acid (GABA) inhibitory neurotransmitters, making these the two the predominant AC populations with each making up close to half of all amacrine cells (Vaney *et al.*, 1990). The adult retina expresses AP-2 $\alpha$  and AP-2 $\beta$  in both the glycinergic and GABAergic amacrine cell populations, with a 77% overlap in their expression profiles (Bassett *et al.*, 2010). Deletion of these two proteins from the developing retina did not appear to influence the genesis of AC in embryonic mouse studies (Bassett *et al.*, 2012). Recently, it has been shown that deletion of AP-2 $\alpha$  and AP-2 $\beta$  from the developing retina at P0 *via* RNAi knockdown experiments, demonstrates a decrease in all amacrine cell populations within the retina by P12 (Jin *et al.*, 2015). In contradiction to

this study, the major amacrine cell populations in both the single and double conditional KO models observed herein did not appear to significantly decrease when measured at 2 months.

GABAergic AC are the first amacrine cell population to arise during retinogenesis, followed by glycinergic AC and a small subset of dopaminergic ACs. GABA transporter 1 (GAT-1) is a reliable indicator of mature AC interneurons, labelling their membranes (Fig. 19). Thus, this marker was used in histological sections from single AP-2 $\alpha$  or AP-2 $\beta$ , and double AP-2 $\alpha$ /AP-2 $\beta$  KO mice to examine the effect the deletion of these proteins may have on the GABAergic population of AC. These studies revealed that there was no significant decrease in GAT-1 immuno-positive cells in any of the conditional knock out strains when compared to controls. Interestingly, there was a significant increase in GAT-1 labelled cells in the  $\alpha$ KI retinas ( $P < 0.0004$ ) (Fig. 20). Cholinergic amacrine cells are one of the earliest born subsets of the GABAergic population (Galli-Resta *et al.*, 1997). The transcription factor Sox2, while expressed in retinal progenitor cells, is a marker for cholinergic ACs and Müller glia (Fig. 19; Lin *et al.*, 2009). Sox2 immuno-labelling showed no significant changes in the population number of this subset of amacrine cells in any of the retinas sampled (Fig. 20). Glycinergic amacrine cells are born later during retinal development, near post-natal day 0. To determine if the deletion of AP-2 $\alpha$  or AP-2 $\beta$  during retinogenesis effects this population of cells in the adult retina, anti-glycine transporter-1 (GLYT-1) was used to stain the membranes of these ACs. When compared with control retinas, there were no significant changes observed in any of the conditional KO mice analyzed (Fig. 21).

Examination of several amacrine cell markers has not revealed significant decrease in any amacrine markers utilized in this study, in single or double conditional knock out mice.

Calretinin is a calcium-binding protein that labels amacrine and ganglion cells in mice (Haverkamp and Wässle, 2000). There was no significant decrease in calretinin-positive cells in any of the conditional knockout retinas, however there was a significant increase in both  $\alpha$ KI ( $P < 0.017$ ) and  $\beta$ KO retinas ( $P < 0.0016$ ). In the double KO and  $\alpha$ KI sections, abnormal sublamina stratification in the IPL was seen. There are five sublaminae within the IPL, and anti-Calretinin marks the three IPL strata at the borders of S1 and S2, S2 and S3, and S3 and S4. These distinct bands of dendrites were completely absent in the double KOs and in sections of the  $\alpha$ KI mutants. The  $\beta$ KO mouse line does not appear to be affected in the deleted regions (Fig. 22).

## **CHAPTER FIVE**

### **Discussion**

Retinogenesis is a complex process requiring precise coordination between intrinsic and extrinsic cues to regulate RPC development into the neurons and glia necessary for vision. Regulatory factors, such as transcription factors have been shown to affect cell fate determination, spatial arrangement, and the synaptic connections between homo- and heterotypic cells of the eye and retina. In particular, AP-2 transcription factors are expressed in many ocular tissues throughout development including the optic cup (West-Mays *et al.*, 1999), developing lens (Pontoriero *et al.*, 2008), corneal epithelium and stroma (Dwivedi *et al.*, 2005), and the neural retina (Bassett *et al.*, 2007; 2010; 2012). In particular, deletion of AP-2 $\alpha$  and AP-2 $\beta$  from the developing murine retina has been shown to disrupt the organization and development of these ocular structures (Bassett *et al.*, 2010; 2012).

Mutations in the human *TFAP2A* and *TFAP2B* genes have been linked to Branchio-oculo facial syndrome (BOFS) and Chare syndrome, respectively. BOFS is an autosomal dominant disorder characterized by ocular and craniofacial defects (Milunsky *et al.*, 2008). Phenotypic abnormalities associated with BOFS are similar to those seen in AP-2 $\alpha$  KO mice which include anophthalmia, microphthalmia, primary aphasia, coloboma of the iris, retina, optic nerve and eyelid (Milunsky *et al.*, 2008; Gestri *et al.*, 2009). BOFS arises from a missense mutation in *TFAP2A* that alters the functional activity of the DNA binding domain. For AP-2, to successfully regulate gene expression it acts as a dimer. Homo- or heterodimerization of a normal protein with mutated AP-2 $\alpha$  can result in a non-functional transcription factor thereby decreasing the overall function of AP-2. Similarly, Char syndrome is an autosomal disorder characterized by facial

dysmorphia, patent ductus arteriosus, and abnormalities of the fifth digit that is associated with missense mutations in *TFAP2B* (Satoda *et al.*, 2000). Identified mutations associated with Char syndrome include missense mutations within the highly conserved basic domain of AP-2 $\beta$ , which impedes the binding of AP-2 $\beta$  to its target sequences, and a missense mutation in the PY motif of the transactivation domain (Satoda *et al.*, 2000; Zhao *et al.*, 2001). Individuals affected by this disorder have striking facial characteristics including wide-set eyes, ptosis, and down-slanting palpebral fissures (Satoda *et al.*, 2000).

### **5.1 AP-2 $\alpha$ and AP-2 $\beta$ Deletion Leads to Downstream Effects in Amacrine Cell Mosaic Patterning**

There is overlapping expression of AP-2 $\alpha$  and AP-2 $\beta$  in the AC populations of embryonic mice, continuing into the post-natal stages (Bassett *et al.*, 2007; 2010). In embryonic studies, abnormal cellular arrangement of cholinergic AC was observed in histological sections immunolabelled with SOX2 and ISL1/2 (Bassett *et al.*, 2012). It has since been shown that *Sox2* plays a role in regulating AC positioning and dendritic stratification in the retina (Whitney *et al.*, 2014). In the present study, post-natal mice lacking AP-2 $\alpha$  and AP-2 $\beta$  expression in the retina exhibited a significant difference in the patterning of cholinergic AC. Together, with the embryonic data, the irregularities observed suggest AP-2 $\alpha$  and AP-2 $\beta$  are involved in organizing a distinct pattern of AC bodies. Along with the aberrant AC patterning, altered sublamination was evident in retinal sections suggesting AP-2 $\alpha$  and AP-2 $\beta$  not only have a role in cell arrangement, but

may also have downstream effects directing the final positioning of their neuronal processes, which cannot occur normally in their absence.

Regular patterning of retinal neurons is essential for proper sampling of the visual field, allowing information to be processed uniformly across the various neurons within the retina. Nearest-neighbour distances and Voronoi domain areas have become the favourable measures of regularity in retinal mosaics, examining the spacing of homotypic cells (Raven *et al.*, 2003; Whitney *et al.*, 2008; 2014). In wild-type mice, there is a mutual repulsion between homotypic cells proximal to one another, which creates exclusion zones, dispersing the neurons throughout the retina (Eglen *et al.*, 2000; 2002). There may be many biological mechanisms that underlie the emergence of these exclusion zones in the developing retina (Raven *et al.*, 2003). In mice lacking AP-2 $\alpha$ , AP-2 $\beta$ , or both AP-2 $\alpha$  and AP-2 $\beta$ , the displaced cholinergic AC residing in the GCL consistently appeared more irregular than those in the INL. This disparity between the two layers is well documented in several mouse lines and has been proposed to be the natural outcome of development in the GCL (Whitney *et al.*, 2008). Early in development cells in the GCL are beneath the growing optic axons, invading retinal astrocytes, and expanding blood vessels. As the eye grows, the retina becomes thinner and the overlying components become intermixed with the cells in the GCL. It was suggested this settling of structures within the GCL disrupts the previously established neuronal mosaics, with a tendency for cells to be aligned along retinal vessels and optic fascicles (Whitney *et al.*, 2008). The cholinergic AC mosaics in the INL, unaffected by the developmental remodelling within the GCL, were also



significantly different in double conditional KOs when compared to controls, suggesting cooperative roles for AP-2 $\alpha$  and AP-2 $\beta$  in retinal mosaic patterning.

The single KO models in this study suggest that deletion of AP-2 $\alpha$  or AP-2 $\beta$  alone is enough to create changes in the mosaic patterning of cholinergic AC in the INL. AP-2 $\alpha$  has been shown in both the embryonic and adult mouse to have similar expression patterns as AP-2 $\beta$  in the AC population (Bassett *et al.*, 2012). AP-2 transcription factors act as homo- or heterodimers to regulate the expression of target genes, with family members able to compensate for deletion of one factor to a certain extent (Bassett *et al.*, 2010). Previous research has shown that in areas where AP-2 $\alpha$  was deleted, and increase in AP-2 $\beta$  expression was observed (Bassett *et al.*, 2007). Due to the compensatory nature of these transcription factors, the deletion of AP-2 $\alpha$  or AP-2 $\beta$  alone does not impede the mosaic patterning of the cholinergic AC significantly such as the loss of both from the retina.

The cholinergic AC in the INL of mice have a distinctly regular distribution, and their patterning is one of the most well studied mosaics in the CNS (Whitney *et al.*, 2014). However, the molecular cues that regulate and maintain this cellular positioning remain poorly understood. During differentiation, AC lose their apico-basal contacts making them more sensitive to environmental stimuli, such as adhesion molecules and transcription factors, in their migratory path (Galli-Resta *et al.*, 2008). Down syndrome cell adhesion molecule (DSCAM) has been shown to prevent cell-cell adhesions, allowing dendrites to migrate to the appropriate destination within the retina (Fuerst *et al.*, 2008; 2009; Keeley *et al.*, 2012) while conditional deletion of DSCAM lead to cell

spacing and dendritic arborisation defects as well as laminar disorganization (Fuerst *et al.*, 2012). Recently, pituitary tumor-transforming gene 1 (Pttg1) expression has been correlated with regular retinal mosaics, with significant decrease in the regularity indexes in retinas where Pttg1 expression is lost (Keeley *et al.*, 2014). AP-2 $\alpha$  has been shown to interact directly with cadherin family members, directly regulating E-cadherin expression in the lens (Pontoriero *et al.*, 2008) and N-cadherin upregulation in corneal cells where AP-2 $\alpha$  is overexpressed (West-Mays *et al.*, 2003). Many members of the cadherin family are found in the retina including R-cadherin, cadherins 6, 7, and 11, and protocadherin (Honjo *et al.*, 2000). It is possible that these retinal-specific cadherins may also be under transcriptional regulation by AP-2 $\alpha$  and AP-2 $\beta$ . AP-2 transcription factors respond to a variety of extracellular signals to subsequently regulate gene expression in several cellular processes including proliferation, apoptosis, and migration (Eckert *et al.*, 2005; Thewes *et al.*, 2010). Loss of nuclear AP-2 $\alpha$  promotes tumor progression, metastasis, and up-regulation of cell-surface adhesion molecules for the motility and invasion of melanoma cells (Leslie & Bar-Eli, 2005). The results in this study suggest that downstream signalling of AP-2 $\alpha$  and AP-2 $\beta$  may regulate the expression of cell adhesion molecules and other factors required for maintaining regular spacing between homotypic neighbouring cells.

Previous studies have suggested AP-2 $\alpha$  and AP-2 $\beta$  play a role in the genetic cascade for AC fate determination and differentiation, with their deletion effecting AC genesis (Jin *et al.*, 2015). The overexpression of AP-2 $\alpha$  and AP-2 $\beta$  was capable of promoting AC development similar to that of Ptf1a, while siRNA knockdown of AP-

2 $\alpha$ /AP-2 $\beta$  expression ablated all AC populations (Jin *et al.*, 2015). Studies from our lab have shown that upon deletion of AP-2 $\alpha$  and AP-2 $\beta$ , AC population size was not affected (Bassett *et al.*, 2012; Zaveri, 2014). For all AC classes examined, GABAergic, glycinergic, and the sub-population of cholinergic AC, no significant decreases in AC numbers were observed in the areas where AP-2 $\alpha$  and AP-2 $\beta$  was deleted in the retinas of our conditional KO mice. The results provided herein suggest AP-2 $\alpha$  and  $\beta$  are not directly involved in the genesis of AC, but do play a role in maintaining their spatial arrangement. The contrariety of these studies may result from the different techniques used to remove the expression of AP-2 $\alpha$  and AP-2 $\beta$  from the retina. Jin *et al.*, utilized electroporation techniques to transfect *Tcfap2a* and *Tcfap2b* shRNAs into the retina to knockdown expression of AP-2 $\alpha$  and AP-2 $\beta$ . Electroporation uses an electric field to generate pores in the membrane, allowing the entry of the shRNA injected into the subretinal space, silencing AP-2 gene expression by RNAi in all cells in which it has permeated. Due to the similarity in sequence of the AP-2 family of genes (Eckert *et al.*, 2005), it is feasible that binding of the shRNA to another family member, such as AP-2 $\gamma$ , may occur. AP-2 $\gamma$  has previously been shown to have overlapping expression with AP-2 $\alpha$  and AP-2 $\beta$  in AC (Bassett *et al.*, 2007; 2010). The KO model studied herein, conditionally deletes expression of AP-2 $\alpha$  and AP-2 $\beta$  from the developing retina. Due to the nature of our model, this expression is deleted in the periphery with the central retina acting as an internal control. It is possible that the residual expression of AP-2 $\alpha$  and AP-2 $\beta$  in the central retina may affect the signalling cascades in the periphery including genesis of AC. As mentioned above, AP-2 $\gamma$  is also expressed in the AC of the murine

retina, and may compensate for the loss of AP-2 $\alpha$  and AP-2 $\beta$  allowing AC genesis to occur as anticipated.

## **5.2 Loss of AP-2 $\alpha$ and AP-2 $\beta$ from the Developing Retina Affects the Physiological Response to Light**

The electroretinogram (ERG) is a powerful, non-invasive tool that measures the retinal response to light. The complex electrical circuitry of the retina is susceptible to signal transmission inhibition detectable by the recorded ERG response (Wässel, 2004). The a-wave measures the functional response of PRs to a light stimulus (Pinto *et al.*, 2007). The recordings from both AP-2 $\alpha$  and AP-2 $\beta$  single KOs, and AP-2 $\alpha$ /AP-2 $\beta$  double KOs had no observable deviations from the a-wave recorded in control mice, suggesting the hyperpolarization of dark-adapted PRs in response to light is unaffected by loss of AP-2 $\alpha$ /AP-2 $\beta$  from the retina. However, transmission of the PR signal forward to the inner retina appeared to be altered by the deletion of AP-2 $\alpha$  and AP-2 $\beta$  resulting in a decrease in b-wave amplitudes

The signal processing response of HC, AC, and BC interneurons post-synaptic to the PRs is recorded as the b-wave in ERGs. The development of proper PR synapse formation is necessary for the transmission of signals from the PRs to BC, and subsequently the inner retina, as well as maintaining retinal lamination of the OPL (Sonntag *et al.*, 2012). When this synapse formation is disrupted, as seen in mice lacking Bassoon, a major component of the PR ribbon synapse, the transfer of signal from PR to post-synaptic cells is inhibited and is reflected in a decrease in the b-wave amplitude in the ERG recording (Dick *et al.*, 2003). The PR ribbon triad appeared to be altered in AP-

2 $\alpha$  and AP-2 $\beta$  KO mice, with spherical ribbon like structures seen in the areas of deletion while control mice and areas of intact AP-2 $\alpha$  and AP-2 $\beta$  expression remained unaltered (Zaveri, 2014). In the double KO mice, the PR ribbon triad changes were seen along with a complete loss of HC (Zaveri, 2014). Horizontal cells are responsible for modulating the signal transmission from PR to BC. When this pathway is compromised, the resulting ERG recordings show a decrease in b-wave amplitudes compared to controls (Sonntag *et al.*, 2012). In the double KOs, we see a large decrease in the amplitudes of b-waves recorded, as expected from the PR synapse remodelling and loss of HC from the retina. Other interneurons of the retina, such as cholinergic AC, contribute to the b-wave response, with changes in the depolarization of cholinergic ACs is known to reduce b-wave amplitudes in dark-adapted mice (Elgueta *et al.*, 2015). In our study, while we see irregular arrangement of cholinergic AC, the population of these cells did not appear to decrease and it is challenging to conclude the effect of the disorganized mosaics on b-wave amplitude. Oscillatory potentials (OPs) appear as four to six wavelets on the rising phase of the ERG b-wave. While the specific cellular origin of OPs is still debated, there is strong evidence that GABAergic neurons and synaptic interactions are key elements in this response (Ramsey *et al.*, 2006). Analyzing these OPs could provide a more confident interpretation of the functional response in those mice with irregularities in their ACs mosaic patterning.

It appears that of the two proteins studied, AP-2 $\beta$  deletion may have a greater effect on retinal function. The b-wave amplitudes of AP-2 $\beta$  single conditional KOs did decrease compared to controls, but not to the same extent as those in the double KO. It

has been shown previously in the adult retina that HC express AP-2 $\beta$  exclusively (Bassett *et al.*, 2010). The loss of AP-2 $\beta$  expression in the single conditional KO may have an effect on this population of cells through alterations to signal transmission from PRs which remains to be elucidated. While AP-2 $\alpha$  deletion appears to have a larger effect on the regularity of AC spacing, it seems to have little influence on the ERG response recorded from the single KO mice. The effects of irregular AC mosaics may be more significant than what was observed in this study alone due to the nature of our conditional KO model and ERG analysis; expression of AP-2 $\alpha$  or AP-2 $\beta$  is only deleted from the peripheral regions of the retina and full field ERGs were used. The central retina in our KO models acts as an internal control, with AP-2 expression unaffected in this region, which may compensate for the AC mosaic irregularities observed in the periphery of these mice. Focal ERGs would allow for the response specific to the regions of deletion to be recorded, giving a more accurate measure of how the function may change.

### **5.3 Conclusions and Future Directions**

This study has shown that while deletion of both AP-2 $\alpha$  and AP-2 $\beta$  does not appear to affect the birth of AC during retinogenesis, it may have downstream effects on the regulation of their mosaic patterning through modulating cell adhesion molecules involved in homotypic interactions determining AC soma and neurite spacing. Due to the changes in neuronal arrangement of AC and loss of HC in AP-2 $\alpha$  and AP-2 $\beta$  KOs, the electrophysiological response to light has been compromised with signals being processed less effectively and efficiently, limiting the output of PRs on the interneurons, disrupting the signals relayed from the GC to the brain. Therefore, this study further

illustrates the careful regulation and interplay between the same set of genes in different aspects of retinal development.

Further work is necessary to fully elucidate the roles of AP-2 $\alpha$  and AP-2 $\beta$  in retinogenesis. The deletion of AP-2 $\alpha$  and AP-2 $\beta$  expression in the retina significantly impedes the regular patterning of cholinergic AC. There are several other subtypes of AC which may also rely on AP-2 $\alpha$  and AP-2 $\beta$  expression for proper cellular arrangement and lamination. Future studies analysing the mosaics of additional AC subtypes would further define the roles of AP-2 $\alpha$  and AP-2 $\beta$  in AC development. Several studies have shown cell adhesion molecules play a major role in regulating the regularity of homotypic cells in the retina, and it is possible these adhesion molecules may be under the control of AP-2 $\alpha$  and AP-2 $\beta$  expression. Studies analyzing the relationship between AP-2 $\alpha$  and AP-2 $\beta$  and the expression of these cell adhesion molecules would provide crucial insight into the genetic cascade regulating cell body positioning and dendritic stratification in the retina. The irregularities observed in the AC mosaic may effect retinal function, which was not ascertained in this study. OPs are thought to be representative of the AC population response in ERGs. Analysis of OPs of conditional KO mice may substantiate a correlation between irregular AC mosaics and the aberrant physiological response to light observed. Studying the role of developmental genes provides important information about the genetic cascades regulating eye formation and increases our understanding of the genes and molecular interactions that may be involved in defects of the eye, such as AP-2. As an extension of the CNS, studying the retina provides insight into the regulatory

cues that are imperative for neuronal development and interactions within neuronal circuitry.



## **REFERENCES**

- Bassett, E.A. *et al.* Overlapping expression patterns and redundant roles for AP-2 transcription factors in the developing mammalian retina. *Dev Dyn* **241**, 814-829 (2012).
- Bassett, E.A. *et al.* Conditional deletion of activating protein 2alpha (AP-2alpha) in the developing retina demonstrates non-cell-autonomous roles for AP-2alpha in optic cup development. *Mol Cell Biol* **27**, 7497-7510 (2007).
- Bassett, E.A. *et al.* AP-2alpha knockout mice exhibit optic cup patterning defects and failure of optic stalk morphogenesis. *Hum Mol Genet* **19**, 1791-1804 (2010).
- Behrens, J., Lowrick, O., Klein-Hitpass, L. & Birchmeier, W. The E-cadherin promoter: Functional analysis of a G.C-rich region and an epithelial cell-specific palindromic regulatory element. *Proc Natl Acad Sci USA* **88**, 11495-11499 (1991).
- Bharti, K., Nguyen, M.-T.T., Skuntz, S., Bertuzzi, S. & Arnheiter, H. The other pigment cell: specification and development of the pigmented epithelium of the vertebrate eye. *Pigment Cell Res* **19**, 380-394 (2006).
- Bok, D. The retinal pigment epithelium: a versatile partner in vision. *J Cell Sci* **17**, 189-195 (1993).
- Brewer, S., Jiang, X., Donaldson, S., Williams, T. & Sucov, H.M. Requirement for AP-2 $\alpha$  in cardiac outflow tract morphogenesis. *Mech Develop* **110**, 139-149 (2002).
- Cepko, C., Austin, C.P., Yang, X., Aleciade, M. & Ezzeddine, D. Cell fate determination in the vertebrate retina. *Proc Natl Acad Sci USA* **93**, 589-595 (1996).
- Cepko, C. Intrinsically different retinal progenitor cells produce specific types of progeny. *Nat Rev Neurosci* **15**, 615-627 (2014).
- Chalepakis, G., Wijnholds, J., Giese, P., Schachner, M. & Gruss, P. Characterization of Pax-6 and Hoxa-1 binding to the promoter region of the Neural Cell Adhesion Molecule L1. *DNA and Cell Biol* **13**, 891-900 (1994).
- Chow, R.L. & Lang, R.A. Early eye development in vertebrates. *Annu Rev Cell Dev Bi* **17**, 255-296 (2001).
- Cvekl, A. & Tamm, E.R. Anterior eye development and ocular mesenchyme: New insights from mouse models and human diseases. *Bioessays* **26**, 374-386 (2004).
- Dick, O. *et al.* The presynaptic active zone protein bassoon is essential for photoreceptor ribbon synapse formation in the retina. *Neuron*. **37**, 775-786 (2003).

- Dong, C.J. & Hare, W.A. Contribution to the kinetics and amplitude of the electroretinogram b-wave by third-order retinal neurons in the rabbit retina. *Vision Res* **40**, 579-589 (2000).
- Dong, C.J. & Hare, W.A. GABA<sub>C</sub> feedback pathway modulates the amplitude and kinetics of ERG b-wave in a mammalian retina in vivo. *Vision Res* **42**, 1081-1087 (2002).
- Dwivedi, D.J. *et al.* Targeted Deletion of AP-2 $\alpha$  Leads to Disruption in Corneal Epithelial Cell Integrity and Defects in the Corneal Stroma. *Invest Ophthalmol Vis Sci* **46**, 3623-3630 (2005).
- Dyer, M.A., Livesey, F.J., Cepko, C.L. & Oliver, G. Prox1 function controls progenitor cell proliferation and horizontal cell genesis in the mammalian retina. *Nat Genet* **34**, 53-58 (2003).
- Eckert, D., Buhl, S., Weber, S., Jager, R. & Schorle, H. The AP-2 family of transcription factors. *Genome Biol* **6**, 246-246.248 (2005).
- Eglen, S.J., van Ooyen, A. & Willshaw, D.J. Lateral cell movement driven by dendritic interactions is sufficient to form retinal mosaics. *Network* **11**, 103-118 (2000).
- Eglen, S.J. & Willshaw, D.J. Influence of cell fate mechanisms upon retinal mosaic formation: a modelling study. *Development* **129**, 5399-5408 (2002).
- Elgueta, C., Vielma, A.H., Palacios, A.G. & Schmachtenberg, O. Acetylcholine induces GABA release onto rod bipolar cells through heteromeric nicotinic receptors expressed in A17 amacrine cells. *Front Cell Neurosci* **9**, 6 (2015).
- Elshatory, Y. *et al.* Islet-1 controls the differentiation of retinal bipolar and cholinergic amacrine cells. *J Neurosci* **27**, 12707-12720 (2007).
- Feng, L. *et al.* Requirement for Bhlhb5 in the specification of amacrine and cone bipolar subtypes in mouse retina. *Development* **133**, 4815-4825 (2006).
- Fuerst, P.G. *et al.* DSCAM and DSCAML1 function in self-avoidance in multiple cell types in the developing mouse retina. *Neuron* **64**, 484-497 (2009).
- Fuerst, P.G., Koizumu, M., Masland, R.H. & Burgess, R.W. Neurite arborization and mosaic spacing in the mouse retina require DSCAM. *Nature* **451**, 470-474 (2008).
- Fujitani, Y. *et al.* Ptf1a determines horizontal and amacrine cell fates during mouse retinal development. *Development* **133**, 4439-4450 (2006).
- Galli-Resta, L. *et al.* The genesis of retinal architecture: an emerging role for mechanical interactions. *Prog Retin Eye Res* **27**, 260-283 (2008).

- Galli-Resta, L. *et al.* Mosaics of Islet-1-expressing amacrine cells assembled by short range cellular interactions. *J Neurosci* **17**, 7831-7838 (1997).
- Gestri, G. *et al.* Reduced TFAP2A function causes variable optic fissure closure and retinal defects and sensitizes eye development to mutations in other morphogenetic regulators. *Hum Genet* **126**, 791-803 (2009).
- Godinho, L. *et al.* Targeting of amacrine cell neurites to appropriate synaptic laminae in the developing zebrafish retina. *Development* **132**, 5069-5079 (2005).
- Hatakeyama, J., Tomita, K., Inoue, T. & Kageyama, R. Roles of homeobox and bHLH genes in specification of retinal cell type. *Development* **128**, 1313-1322 (2001).
- Haverkamp, S. & Wässle, H. Immunocytochemical analysis of the mouse retina. *J Comp Neurol* **424**, 1-23 (2000).
- Hilger-Eversheim, K., Moser, M., Schorle, H. & Buettner, R. Regulatory roles of AP-2 transcription factors in vertebrate development, apoptosis, and cell-cycle control. *Gene* **260**, 1-12 (2000).
- Honjo, M. *et al.* Differential expression of cadherin adhesion receptors in neural retina of the postnatal mouse. *Invest Ophthalmol Vis Sci*. **41**, 546-551 (2000).
- Hoon, M., Okawa, H., Della Santina, L. & Wong, R.O. Functional architecture of the retina: development and disease. *Prog Retin Eye Res* **42**, 44-84 (2014).
- Inoue, T. *et al.* Math3 and NeuroD regulate amacrine cell fate specification in the retina. *Development* **129**, 831-842 (2002).
- Jin, K. *et al.* Tfp2a and 2b act downstream of Ptf1a to promote amacrine cell differentiation during retinogenesis. *Mol Brain* **8**, 28 (2015).
- Keeley, P. W. *et al.* Pituitary tumor-transforming gene 1 regulates the patterning of retinal mosaics. *Proc Natl Acad Sci USA* **111**, 9295-9300 (2014).
- Keeley, P.W. *et al.* Neuronal clustering and fasciculation phenotype in Dscam- and Bax-deficient mouse retinas. *J Comp Neurol* **520**, 1349-1364 (2012).
- Kolb, H. How the Retina Works. *American Scientist* **91**, 28-35 (2003).
- Lefebvre, J.L., Kostadinov, D., Chen, W.V., Maniatis, T. & Sanes, J.R. Protocadherins mediate dendritic self-avoidance in the mammalian nervous system. *Nature* **488**, 517-521 (2012).

- Lefebvre, J.L., Zhang, Y., Meister, M., Wang, X. & Sanes, J.R. gamma-Protocadherins regulate neuronal survival but are dispensable for circuit formation in retina. *Development* **135**, 4141-4151 (2008).
- Leslie, M.C. & Bar-Eli, M. Regulation of gene expression in melanoma: new approaches for treatment. *J Cell Biochem* **94**, 25-38 (2005).
- Levine, E.M. & Green, E.S. Cell-intrinsic regulators of proliferation in vertebrate retinal progenitors. *Semin Cell Dev Biol* **15**, 63-74 (2004).
- Li, Q. & Dashwood, R.H. Activator Protein 2a Associates with Adenomatous Polyposis Coli/B-Catenin and inhibits B-Catenin/T-cell Factor Transcriptional Activity in Colorectal Cancer Cells. *J. Biol. Chem.* **279**, 45669-45675 (2004).
- Li, S. *et al.* Foxn4 controls the genesis of amacrine and horizontal cells by retinal progenitors. *Neuron* **43**, 795-807 (2004).
- Li, X., Glubrecht, D.D. & Godbout, R. AP2 transcription factor induces apoptosis in retinoblastoma cells. *Gene Chromosome Canc* **49**, 819-830 (2010).
- Li, X., Monckton, E.A. & Godbout, R. Ectopic expression of transcription factor AP-2delta in developing retina: effect on PSA-NCAM and axon routing. *J Neurochem* **129**, 72-84 (2014).
- Lin, Y.P., Ouchi, Y., Satoh, S. & Watanabe, S. Sox2 plays a role in the induction of amacrine and Muller glial cells in mouse retinal progenitor cells. *Invest Ophthalmol Vis Sci* **50**, 68-74 (2009).
- Livesey, F.J. & Cepko, C.L. Vertebrate Neural Cell-Fate Determination: Lessons From the Retina. *Nat Rev Neurosci* **2**, 109-118 (2001).
- Marquardt, T. Transcriptional control of neuronal diversification in the retina. *Prog Retin Eye Res* **22**, 567-577 (2003).
- Marquardt, T., Ashery-Padan, R., Andrejewski, N., Scardigli, R. & Guillemot, F.G., P. Pax6 is required for the multipotent state of retinal progenitor cells. *Cell* **105**, 43-55 (2001).
- Martinez-Morales, J.R., Rodrigo, I. & Bovolenta, P. Eye development: a view from the retina pigmented epithelium. *Bioessays* **26**, 766-777 (2004).
- Matsuoka, R.L. *et al.* Transmembrane semaphorin signalling controls laminar stratification in the mammalian retina. *Nature* **470**, 259-263 (2011).
- Milunsky, J.M. *et al.* TFAP2A mutations result in branchio-oculo-facial syndrome. *Am J Hum Genet* **82**, 1171-1177 (2008).

- Mo, Z., Li, S., Yang, X. & Xiang, M. Role of the Barhl2 homeobox gene in the specification of glycinergic amacrine cells. *Development* **131**, 1607-1618 (2004).
- Moser, M. *et al.* Cloning and characterization of a second AP-2 transcription factor: AP-2 $\beta$ . *Development* **121**, 2779-2788 (1995).
- Moser, M. *et al.* Enhanced apoptotic cell death of renal epithelial cells in mice lacking transcription factor AP-2 $\beta$ . *Gene Dev* **11**, 1938-1948 (1997).
- Nir, I. *et al.* Dysfunctional light-evoked regulation of cAMP in photoreceptors and abnormal retinal adaptation in mice lacking dopamine D4 receptors. *J Neurosci* **22**, 2063-2073 (2002).
- Pinto, L.H., Invergo, B., Shimomura, K., Takahashi, J.S. & Troy, J.B. Interpretation of the mouse electroretinogram. *Doc Ophthalmol* **115**, 127-136 (2007).
- Poche, R.A. *et al.* Lim1 is essential for the correct laminar positioning of retinal horizontal cells. *J Neurosci* **27**, 14099-14107 (2007).
- Poche, R.A. & Reese, B.E. Retinal horizontal cells: challenging paradigms of neural development and cancer biology. *Development* **136**, 2141-2151 (2009).
- Pontoriero, G.F. *et al.* Cell Autonomous Roles for AP-2 $\alpha$  in Lens Vesicle Separation and Maintenance of the Lens Epithelial Cell Phenotype. *Dev Dyn* **237**, 602-612 (2008).
- Ramsey, D. J., Ripps, H. & Qian, H. An electrophysiological study of retinal function in the diabetic female rat. *Invest Ophthalmol Vis Sci* **47**, 5116-5124, doi:10.1167/iovs.06-0364 (2006).
- Raven, M.A., Eglén, S.J., Ohab, J.J. & Reese, B.E. Determinants of the exclusion zone in dopaminergic amacrine cell mosaics. *J Comp Neurol* **461**, 123-136 (2003).
- Reese, B.E. & Galli-Resta, L. The role of tangential dispersion in retinal mosaic formation. *Prog Retin Eye Res* **21**, 153-168 (2002).
- Reese, B.E. & Keeley, P.W. Design principles and developmental mechanisms underlying retinal mosaics. *Biol Rev Camb Philos Soc* **90**, 854-876 (2015).
- Reese, B.E. & Keeley, P.W. Genomic control of neuronal demographics in the retina. *Prog Retin Eye Res* **55**, 246-259 (2016).
- Satoda, M. *et al.* Mutations in TFAP2B cause Char syndrome, a familial form of patent ductus arteriosus. *Nat Genet* **25**, 42-46 (2000).

Sieving, P. A. 'Unilateral cone dystrophy': ERG changes implicate abnormal signaling by hyperpolarizing bipolar and/or horizontal cells. *Trans Am Ophthalmol Soc.* 92, 459-471 (1994).

Smith, R.S. & Kao, W.W.Y.J., S.W.M. *Systematic Evaluation of the Mouse Eye: Anatomy, Pathology, and Biomethods.* (CRC Press, 2002).

Sonntag, S. *et al.* Ablation of retinal horizontal cells from adult mice leads to rod degeneration and remodeling in the outer retina. *J Neurosci* **32**, 10713-10724 (2012).

Sun, L.O. *et al.* On and off retinal circuit assembly by divergent molecular mechanisms. *Science* **342**, 1241974 (2013).

Thewes, V. *et al.* Interference with activator protein-2 transcription factors leads to induction of apoptosis and an increase in chemo- and radiation-sensitivity in breast cancer cells. *BMC Cancer* **10**, 192 (2010).

Tian, N. & Slaughter, M.M. Correlation of dynamic responses in the ON bipolar neuron and the b-wave of the electroretinogram. *Vision Res* **35**, 1359-1364 (1995).

Trimarchi, J.M., Stadler, M.B. & Cepko, C.L. Individual retinal progenitor cells display extensive heterogeneity of gene expression. *PLoS One* **3**, e1588 (2008).

Vaney, D.I. The mosaic of amacrine cells in the mammalian retina. *Prog Ret Res* **9**, 49-100 (1990).

Wässle, H. Parallel processing in the mammalian retina. *Nat Rev Neurosci* **5**, 747-757 (2004).

West-Mays, J.A. *et al.* Positive influence of AP-2alpha transcription factor on cadherin gene expression and differentiation of the ocular surface. *Differentiation* **71**, 206-216 (2003).

West-Mays, J.A. *et al.* AP-2 $\alpha$  transcription factor is required for early morphogenesis of lens vesicle. *Dev Biol* **206**, 46-62 (1999).

Whitney, I.E., Keeley, P.W., Raven, M.A. & Reese, B.E. Spatial patterning of cholinergic amacrine cells in the mouse retina. *J Comp Neurol* **508**, 1-12 (2008).

Whitney, I.E. *et al.* Sox2 regulates cholinergic amacrine cell positioning and dendritic stratification in the retina. *J Neurosci* **34**, 10109-10121 (2014).

Wong, R.O.L. & Godinho, L. *Development of the Vertebrate Retina.* (MIT Press, Cambridge; 2004).

Wu, F. *et al.* Onecut1 is essential for horizontal cell genesis and retinal integrity. *J Neurosci* **33**, 13053-13065, 13065a (2013).

Xiang, M. Intrinsic control of mammalian retinogenesis. *Cell Mol Life Sci* **70**, 2519-2532 (2013).

Xiang, M. & Li, S. Foxn4: a multi-faceted transcriptional regulator of cell fates in vertebrate development. *Sci China Life Sci* **56**, 985-993 (2013).

Zaveri M. The role of AP-2 $\alpha$  and AP-2 $\beta$  in horizontal cell development and amacrine cell patterning.: McMaster University (2014).

Zhang, X., Serb, J.M. & Greenlee, M.H. Mouse retinal development: a dark horse model for systems biology research. *Bioinform Biol Insights* **5**, 99-113 (2011).

Zhao, F. *et al.* Novel TFAP2B mutations that cause Char syndrome provide a genotype-phenotype correlation. *Am J Hum Genet* **69**, 695-703 (2001).

Zhu, C.H., Huang, Y., Oberley, L.W. & Domann, F.E. A family of AP-2 proteins down-regulate manganese superoxide dismutase expression. *J Biol Chem* **276**, 14407-14413 (2001).



## **FIGURES**

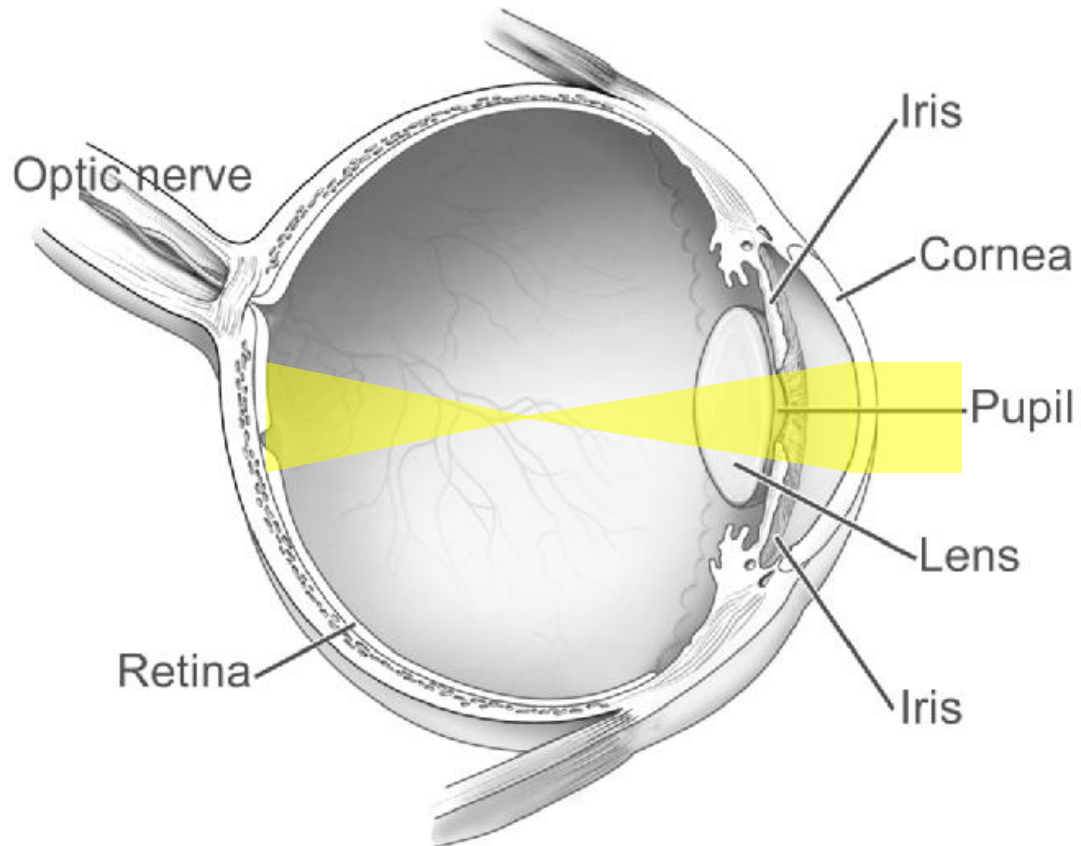


**Figure 1. The eye.** As light passes through the cornea, it is focused on the retina *via* the transparent lens. The retina, the nerve layer at the back of the eye necessary for vision, senses this light and sends an electrical signal down the optic nerve into the brain. The vitreous humour is a clear, gelatinous substance that fills the space in the posterior chamber. Regulation of light admittance is controlled by the iris and pupil. Adapted from [www.nei.nih.gov](http://www.nei.nih.gov).

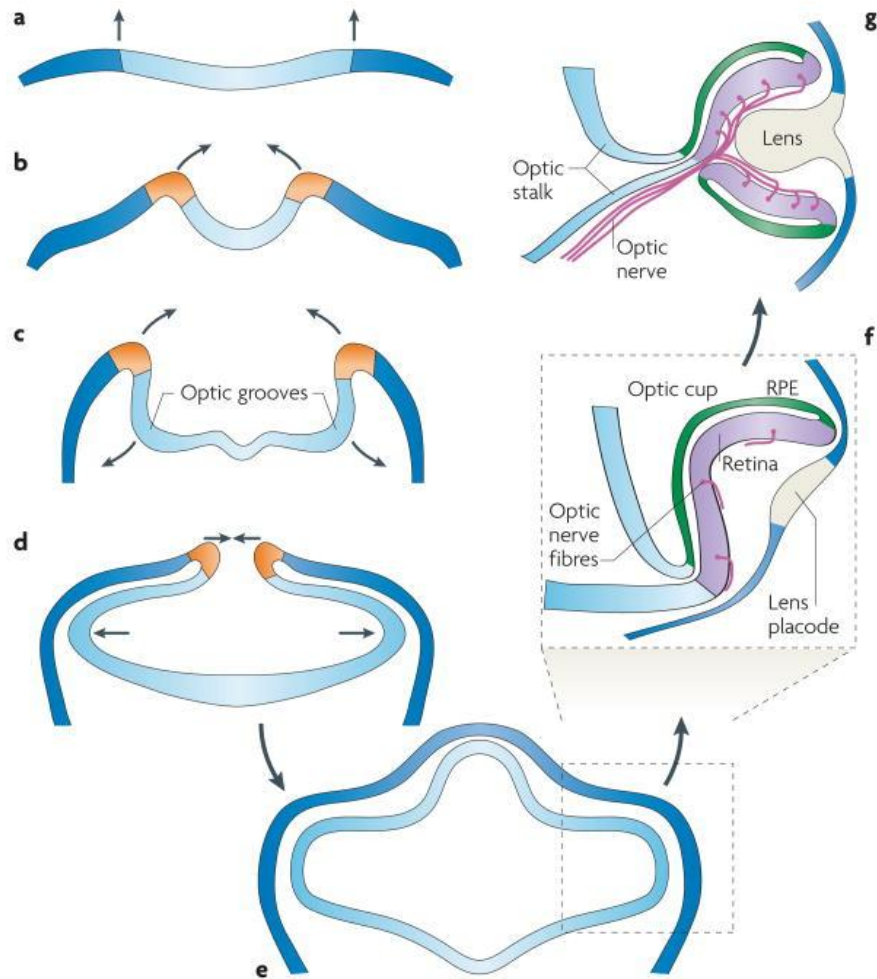


**Figure 2. Vertebrate eye development.** Development of the vertebrate eye cup begins when the neural tube folds upwards (a) and inwards (b), followed by the evagination of the optic grooves (c). The neural folds approach each other as the optic vesicles bulge outwards (d), with the neural tube pinching off after sealed (e). The optic vesicles continue to push outwards, eventually contacting the surface ectoderm causing induction of the lens placode. The lens placode (f) pinches off to form the lens vesicle. The optic vesicles invaginate, forming the optic cup which will give rise to the RPE and neural retina (g). Adapted from Lamb *et al.*, 2007.

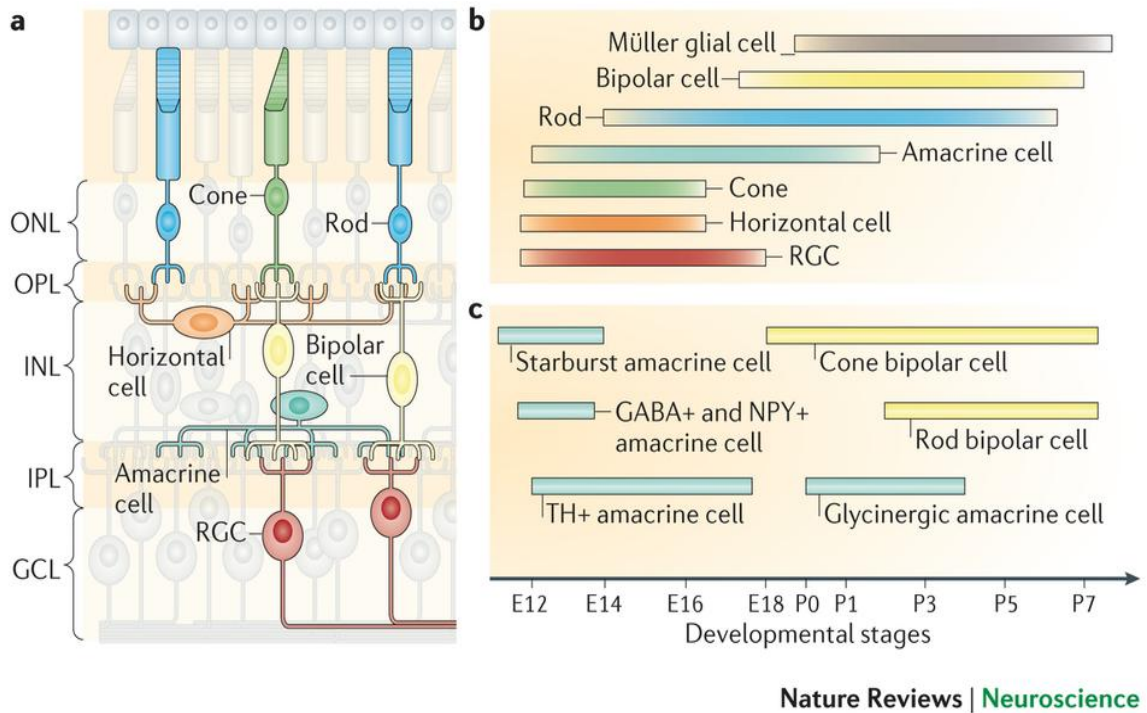


**Figure 3. Retinal development.** (A) The retina has three distinct layers of neuron cell bodies, the outer nuclear layer (ONL), inner nuclear layer (INL) and ganglion cell layer (GCL). Two synaptic layers, the outer plexiform layer (OPL) and inner plexiform layer (IPL). Retinal neurons are comprised of primary sensory neurons (rod and cone photoreceptors), interneurons (horizontal, bipolar, and amacrine cells), and the output neurons (ganglion cells). (B) Retinal neurons are born in a fixed, overlapping chronological order. The birth dates of each of the major cell types for rat and mouse are shown. Adapted from Cepko, 2014.

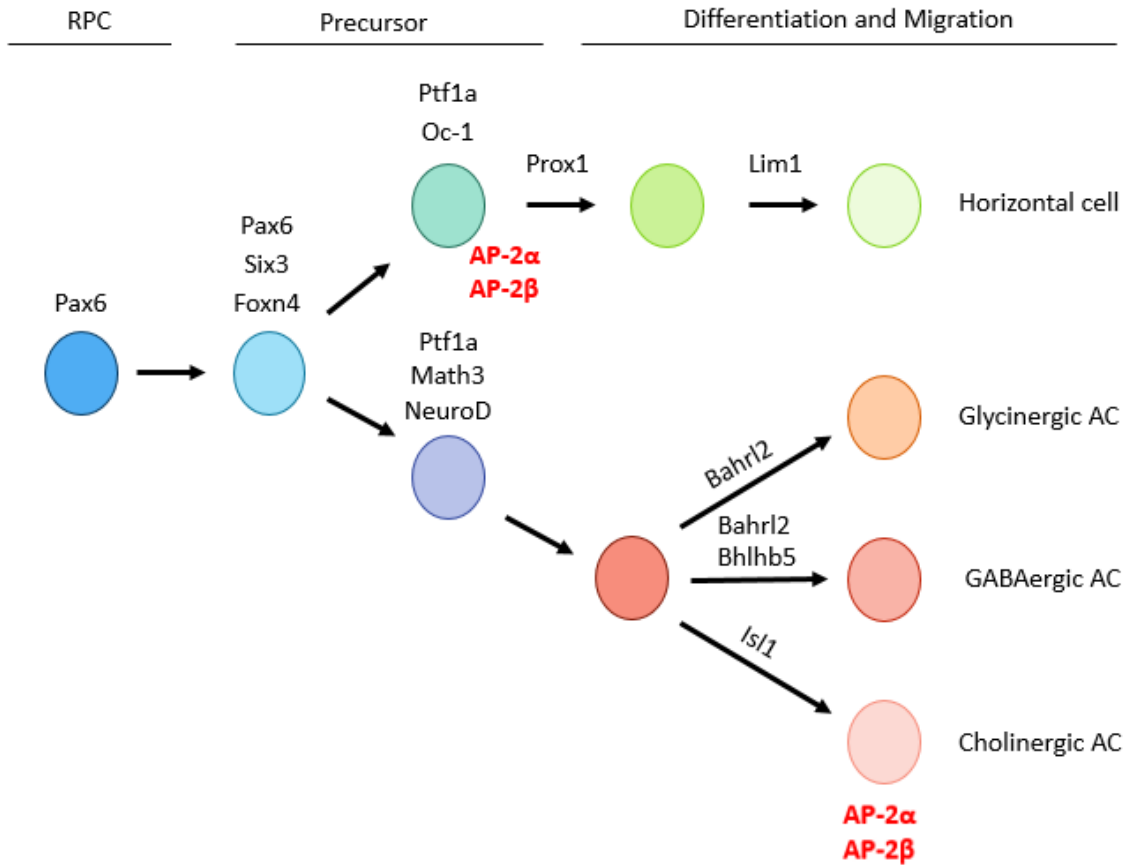


**Figure 4. The transcriptional cascades regulating amacrine and horizontal cell development.** The expression of early transcription factors Pax6 and Foxn4 allow the retinal progenitor cells to begin the path toward development into horizontal and amacrine cells. Parallel pathways of Onecut and Ptf1a, followed by Prox1 lead to HC genesis, with Lim1 modulating its cellular arrangement. Previous work has suggested AP-2 $\alpha$ /AP-2 $\beta$  plays a redundant role in this path. Ptf1a expression with Math3 or NeuroD leads to AC genesis, with a number of transcription factors responsible for differentiation into the various AC types. We have proposed AP-2 $\alpha$ /AP-2 $\beta$  are not responsible for AC differentiation, instead regulate their cellular mosaic arrangement. Modified from Fujitani *et al.*, 2006; Poche & Reese, 2009.

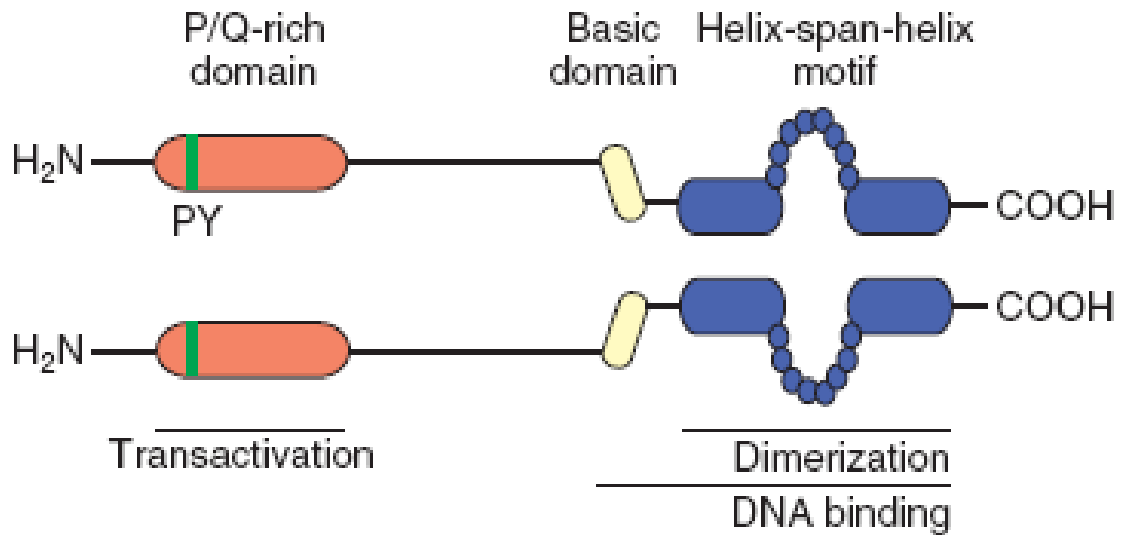


**Figure 5. Activating Protein-2.** Schematic representation of the protein structure of an AP-2 dimer including the proline- glutamine- rich transactivation domain (PQ), helix-span-helix domain, responsible for dimerization and the basic domain which mediates DNA binding together with the helix-span-helix motif. Adapted from Eckert *et al.*, 2005

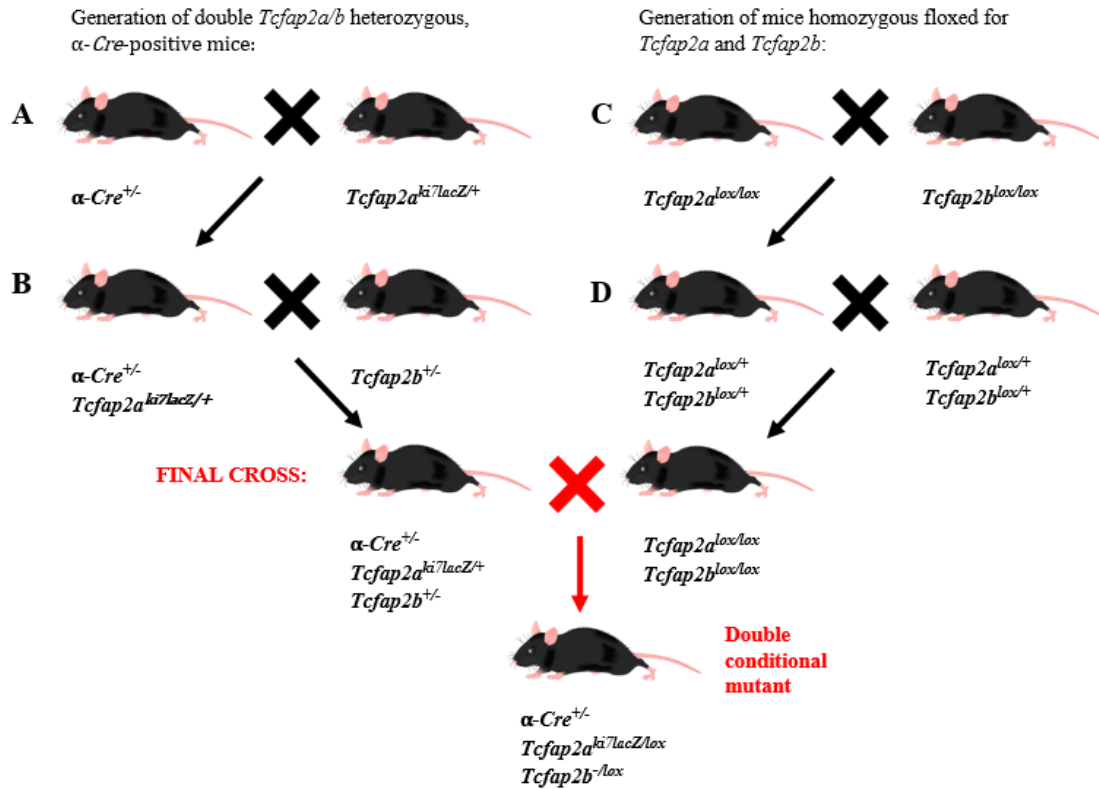


**Figure 6. Generation of double conditional *Tcfap2a/Tcfap2b* mutants.** (A)  $\alpha$ -Cre transgenic mice expressing Cre recombinase under the “Pax6  $\alpha$  enhancer” are crossed with mice heterozygous for the *Tcfap2a* gene. (B) The resulting  $\alpha$ -Cre<sup>+/-</sup>/*Tcfap2a*<sup>ki7lacZ/+</sup> mice are bred with mice heterozygous for the *Tcfap2b* gene, generating mice with one copy of each *Tcfap2* allele and the presence of Cre-recombinase:  $\alpha$ -Cre<sup>+/-</sup>/*Tcfap2a*<sup>ki7lacZ/+</sup>/*Tcfap2b*<sup>+/-</sup>. (C) In a separate set of crosses, homozygous floxed *Tcfap2a* and *Tcfap2b* were paired together and their resulting heterozygous floxed offspring (D) were interbred to regain homozygosity: *Tcfap2a*<sup>lox/lox</sup>/*Tcfap2b*<sup>lox/lox</sup>. The final cross paired the floxed mice with the Cre/*Tcfap2* heterozygotes, resulting in double conditional mutants:  $\alpha$ -Cre/*Tcfap2a*<sup>ki7lacZ/lox</sup>/*Tcfap2b*<sup>-/lox</sup>.

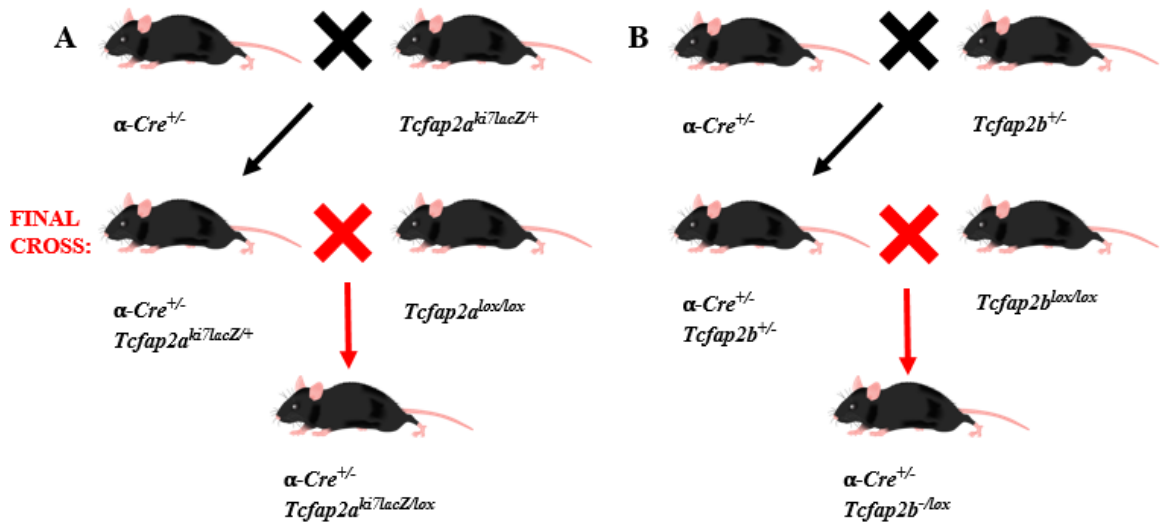


**Figure 7. Generation of single conditional *Tcfap2a* and *Tcfap2b* mutants.** (A)  $\alpha$ -Cre transgenic mice were bred with heterozygous *Tcfap2a* mice. The resulting offspring,  $\alpha\text{-Cre}^{+/-}/Tcfap2a^{ki7lacZ/+}$  were crossed with mice homozygous for the *Tcfap2a*<sup>lox</sup> allele to produce mice conditional *Tcfap2a* mutants:  $\alpha\text{-Cre}/Tcfap2a^{ki7lacZ/lox}$ . (B) In a similar set of crosses, the same Cre transgenic mice were bred with mice heterozygous for the *Tcfap2b* gene. These  $\alpha\text{-Cre}/Tcfap2b^{+/-}$  mice were bred with homozygous *Tcfap2b*<sup>lox</sup> mice to generate offspring with *Tcfap2b* conditionally deleted from the retina:  $\alpha\text{-Cre}^{+/-}/Tcfap2b^{-/lox}$ .



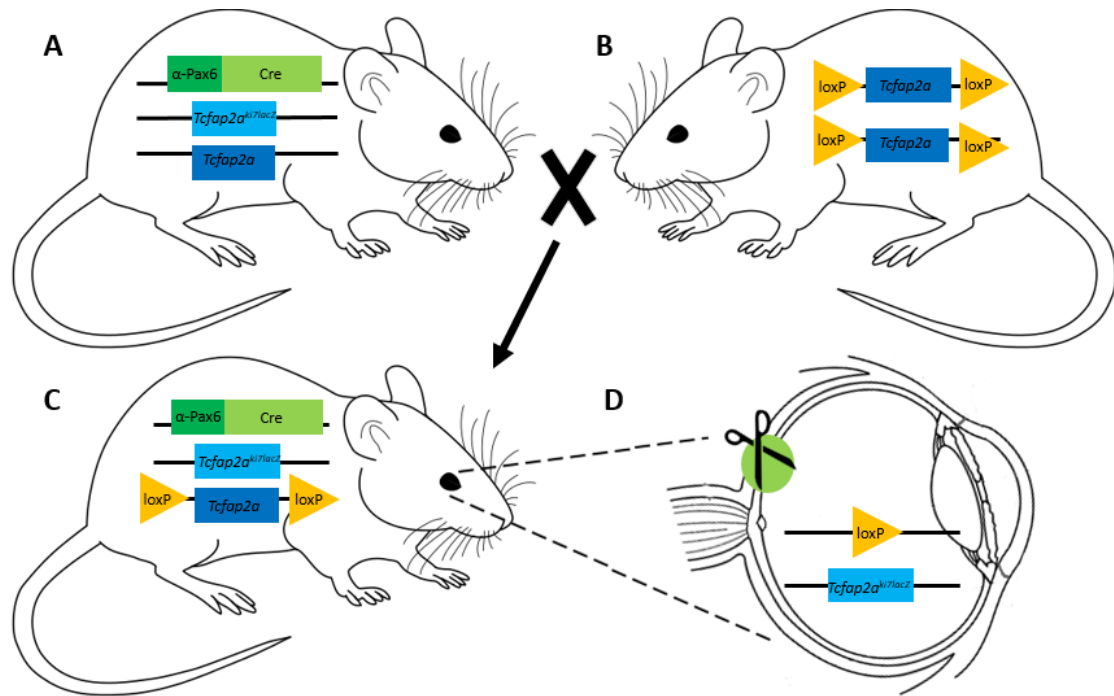


**Figure 8. Cre-loxP tissue specific deletion.** (A) Mice heterozygous for the Cre-transgene and *Tcfap2a*<sup>ki7lacZ</sup> and mice with *Tcfap2a* homozygous floxed (B) were crossed together. (C) The resulting mice carry Cre-recombinase under the Pax6  $\alpha$ -enhancer, one *Tcfap2a* allele germ-line deleted and the other *Tcfap2a* allele flanked with loxP sites. (D) The floxed *Tcfap2a* allele is excised by the Cre-recombinase in any area the Pax6  $\alpha$ -enhancer is activated, thereby conditionally deleting AP-2 $\alpha$  expression in the developing retina. (Adapted from Jackson Laboratories, <https://www.jax.org>).

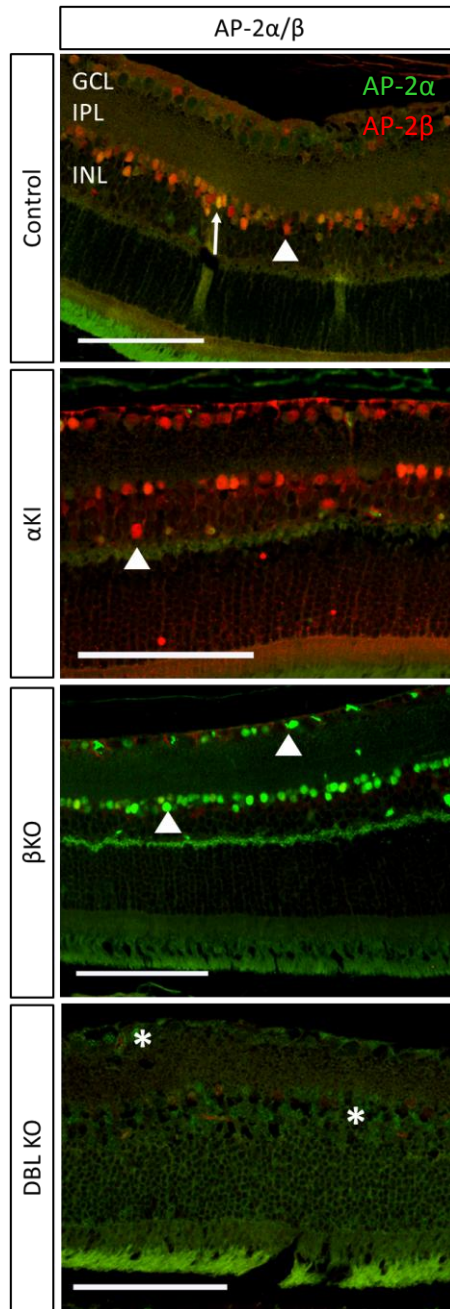


**Figure 9. Expression of AP-2 $\alpha$ /AP-2 $\beta$  in the retina.** AP-2 $\alpha$  and AP-2 $\beta$  exhibit overlapping expression patterns in the adult mouse retina (arrow). Both proteins are expressed in the INL where horizontal and amacrine cells reside, and they are expressed in displaced amacrine cells in the GCL (arrowheads). This expression is completely lost in the AP-2 $\alpha$ / $\beta$  DBL KO (\*). Loss of AP-2 $\alpha$  expression in  $\alpha$ KI and AP-2 $\beta$  in  $\beta$ KO mice did not affect the expression of the other marker. GCL, ganglion cell layer; IPL, inner plexiform layer; INL, inner nuclear layer. Scalebars: 100 $\mu$ m

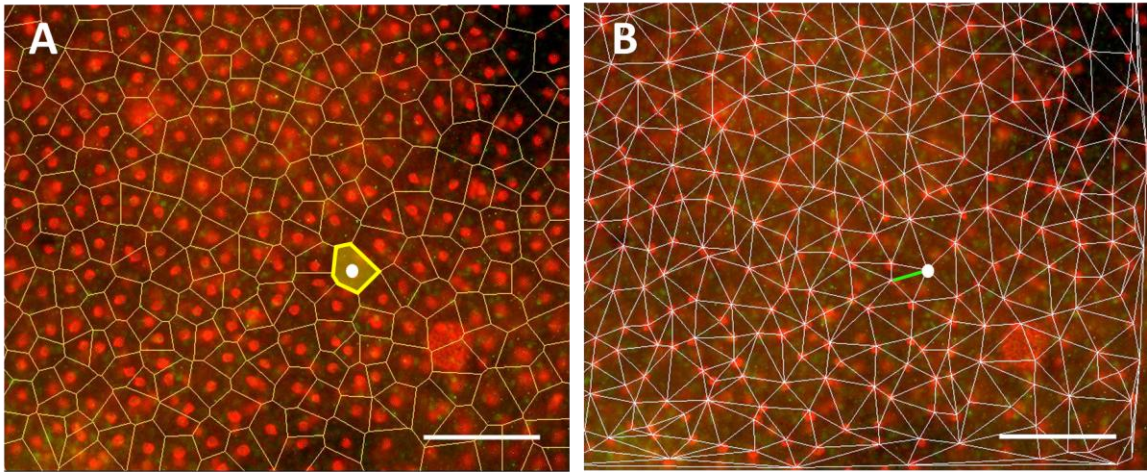


**Figure 10. Voronoi domain areas and nearest-neighbour distances.** Flat mount retinas were stained with anti-ChAT (red) and anti-AP-2 $\alpha$  (green) for Voronoi domain and nearest-neighbour spatial analyses. (A) Voronoi domain determines the area of points in the retina that are closest to one cell than any other cell (outlined in yellow). (B) Nearest-neighbour analyses of the same cell determines the shortest distance between cholinergic AC (indicated in green). Scale bars: 100 $\mu$ m

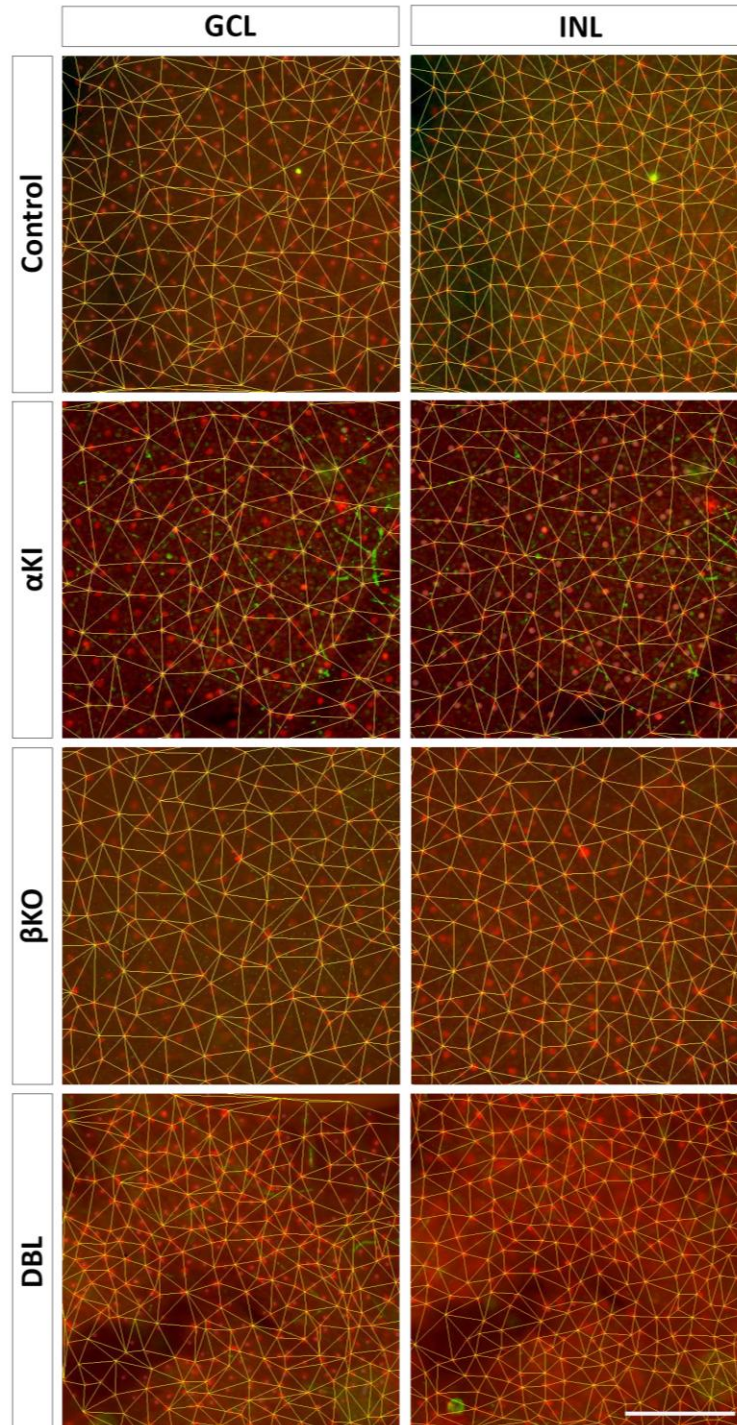


**Figure 11. Representative nearest-neighbour distances in single and double KO mice retinas.** Retinal flat mounts were stained with ChAT (red) to visualize cholinergic amacrine cells. Nearest-neighbour distances (yellow), were determined using FIJI software (NIH). Scale bar: 100  $\mu\text{m}$

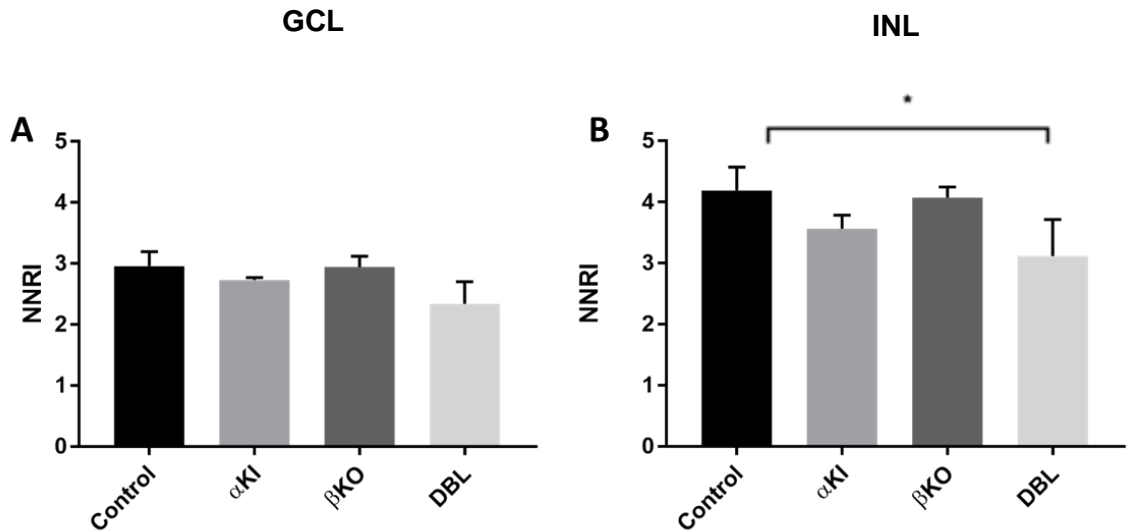


**Figure 12. Decreased regularity in nearest-neighbour distances in double conditional KOs.** (A) No significant changes were seen in the Voronoi domain regularity index (VDRI) in the GCL of either single KO or the double KO models. (B) A marked decrease in NNRI was seen in the INL of DBL KO mice ( $3.12 \pm 0.60$ ) compared with controls ( $4.19 \pm 0.39$ ). (Mean  $\pm$  SD, 4 retinas per group; \* $P < 0.03$ , one-way ANOVA with Bonferroni multiple comparisons test).

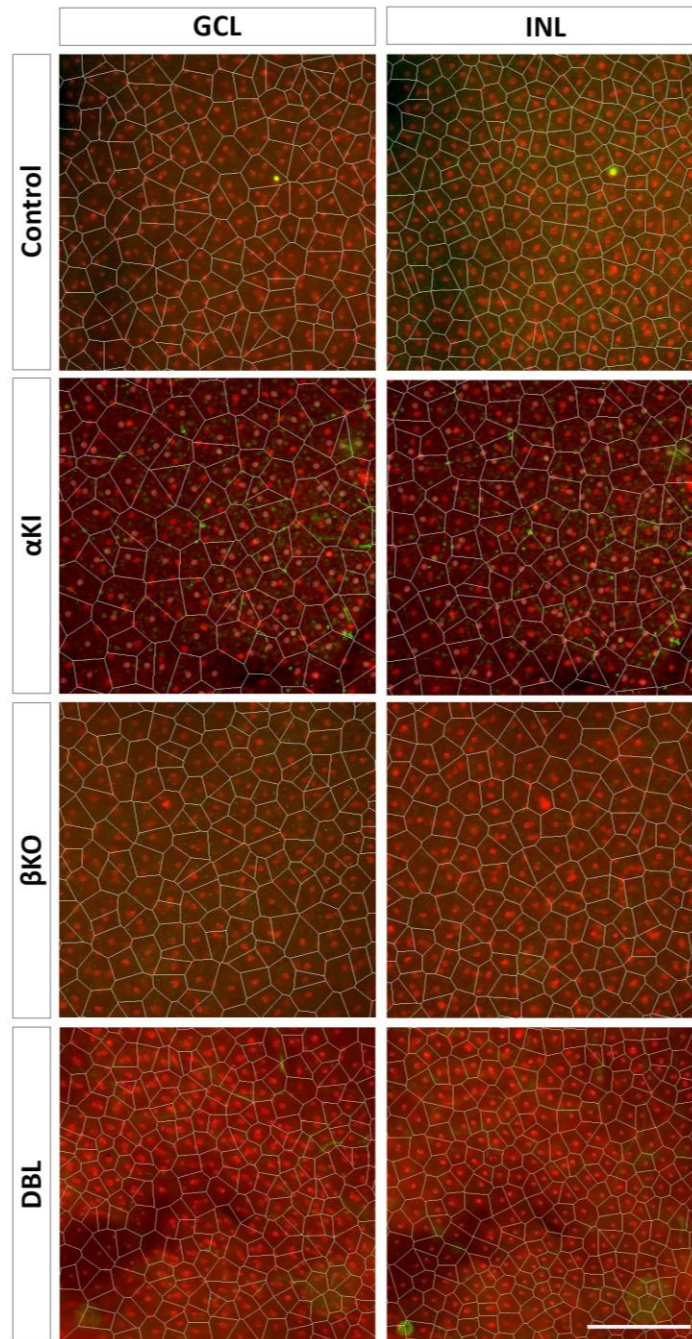


**Figure 13. Representative Voronoi domain areas for single and double KO mice retinas.** Retinal flat mounts were stained with ChAT (red) to visualize cholinergic amacrine cells. Voronoi domain areas (bound in white), were determined using FIJI software (NIH). Scale bar: 100  $\mu\text{m}$

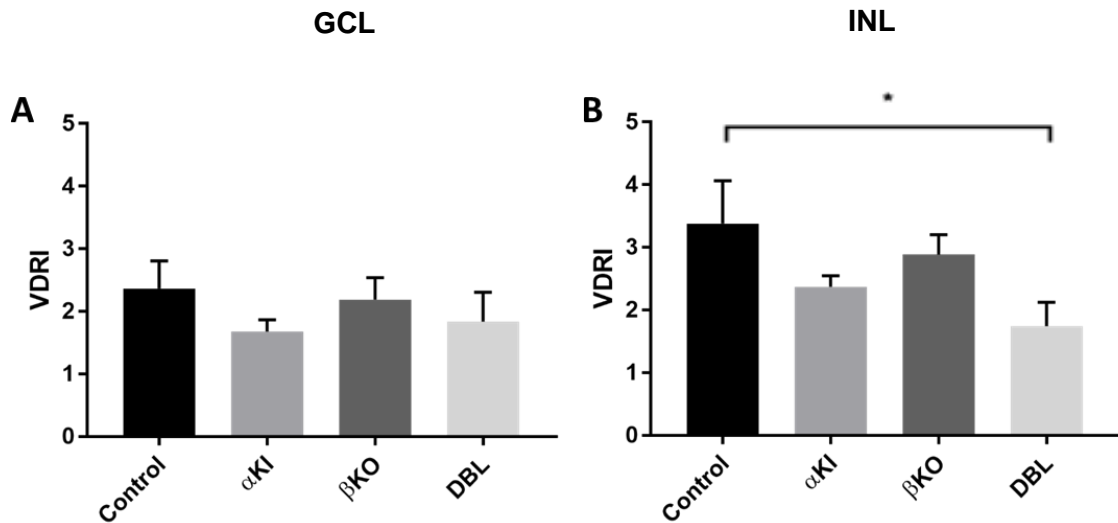


**Figure 14. Decreased Voronoi domain regularity index in the INL of  $\alpha$ KI and DBL KO mice.** (A) No significant changes were seen in the Voronoi domain regularity index (VDRI) in the GCL of either single KO or the double KO models. (B) A significant reduction in the VDRI in the INL of DBL KO mice ( $1.75 \pm 0.38$ ) compared with controls ( $3.38 \pm 0.68$ ) was observed. (Mean  $\pm$  SD, 4 retinas per group; \* $P < 0.01$ , one-way ANOVA with Bonferroni multiple comparisons test).

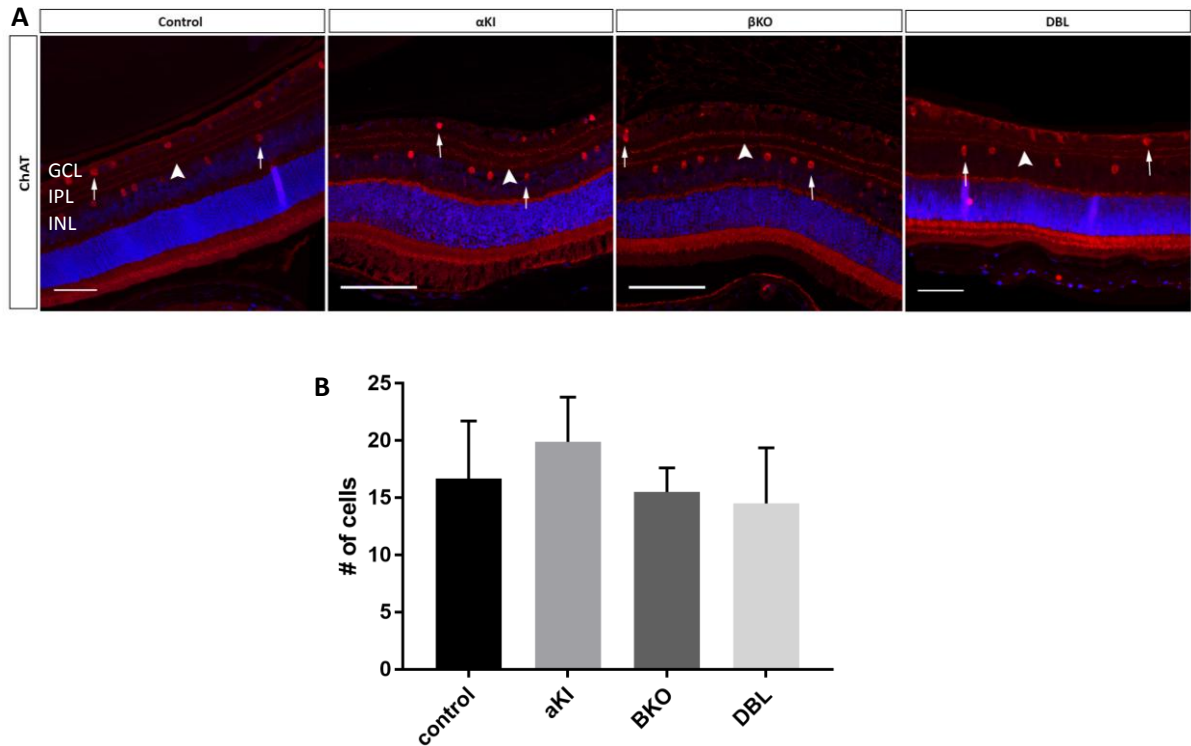


**Figure 15. Cholinergic amacrine cells in the INL and GCL of conditional KO mice remain unchanged.** (A) No irregularities in cholinergic amacrine cell arrangement could be derived from these sections (arrows), and synaptic staining in the IPL remained consistent across all animals studied (arrowheads). (B) Quantification of cells immunoreactive for ChAT in the periphery of histological sections at 2 months (shown as the mean  $\pm$  SD for 3 retinas per group). In all sections analyzed, the number of ChAT-positive AC did not significantly differ from control values. (Mean  $\pm$  SD, 3 retinas per group;  $P > 0.05$ , one-way ANOVA with Bonferroni multiple comparison tests). Scalebars: 100 $\mu$ m



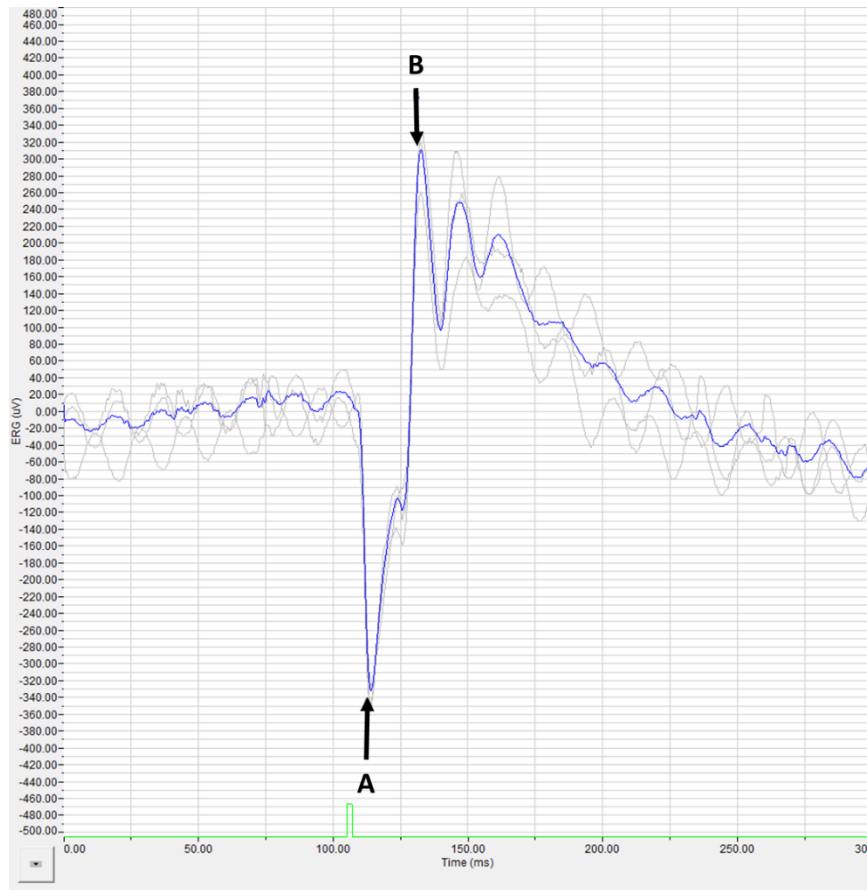


**Figure 16. Representative dark-adapted, full field electroretinogram response.** When anesthetized animals, with body temperature maintained at 37°C, were stimulated with light (504nm), the evoked response was recorded and a- and b-wave amplitudes measured. The a-wave is derived from the hyperpolarization of PR in response to light with its amplitude measured from baseline to trough. The b-wave is derived from the depolarization of neurons in the inner retina, and its amplitude is measured from the trough of the a-wave to the peak of the b-wave.

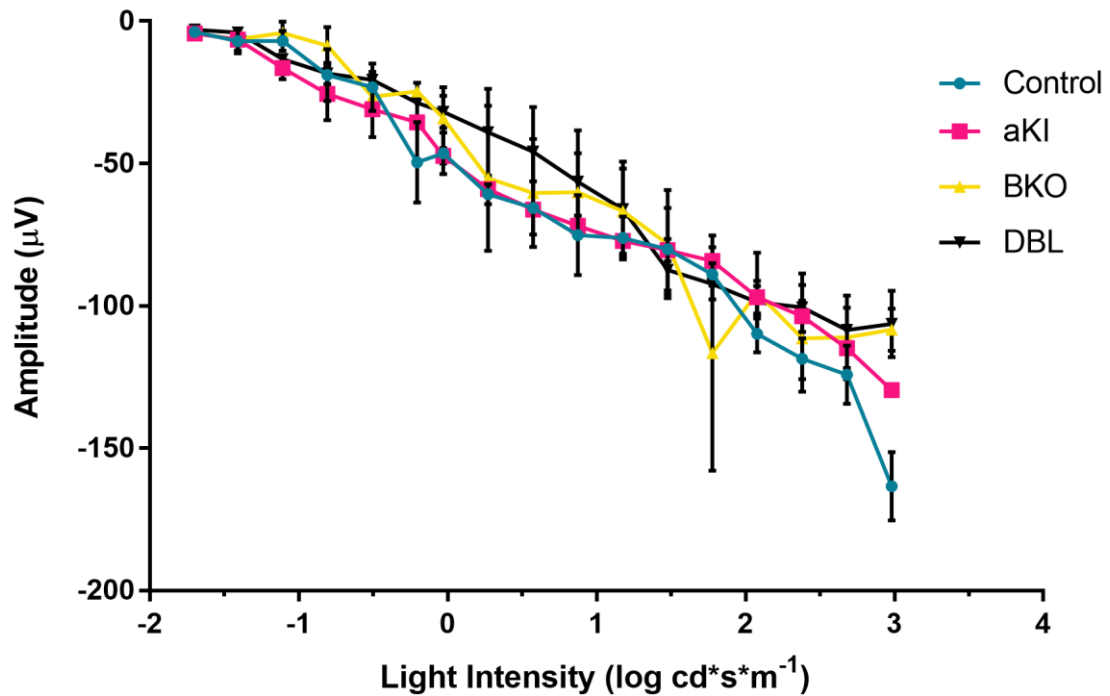


**Figure 17. A-wave amplitudes decrease with increasing flash intensities.** As flash intensities of light (504 nm) were increased, the a-wave decreased in a relative fashion, with flash intensity repeated measures yielding significantly different amplitudes ( $F_{16,128}=1626$ ,  $P<0.0001$ ). All groups tested,  $\alpha$ KI (pink),  $\beta$ KO (yellow) and double KO mice (black), showed a similar pattern to that seen in control mice (blue). The hyperpolarization of photoreceptors, as represented by this a-wave, appears to be maintained regardless of deletion of AP-2 $\alpha$ , AP-2 $\beta$ , or AP-2 $\alpha/\beta$  from the retina. No significant deviance from controls was observed. (Mean  $\pm$  SD, 3 eyes analyzed per group. Two-way repeated-measures ANOVA with Tukey's HSD post-hoc analysis between genotypes).

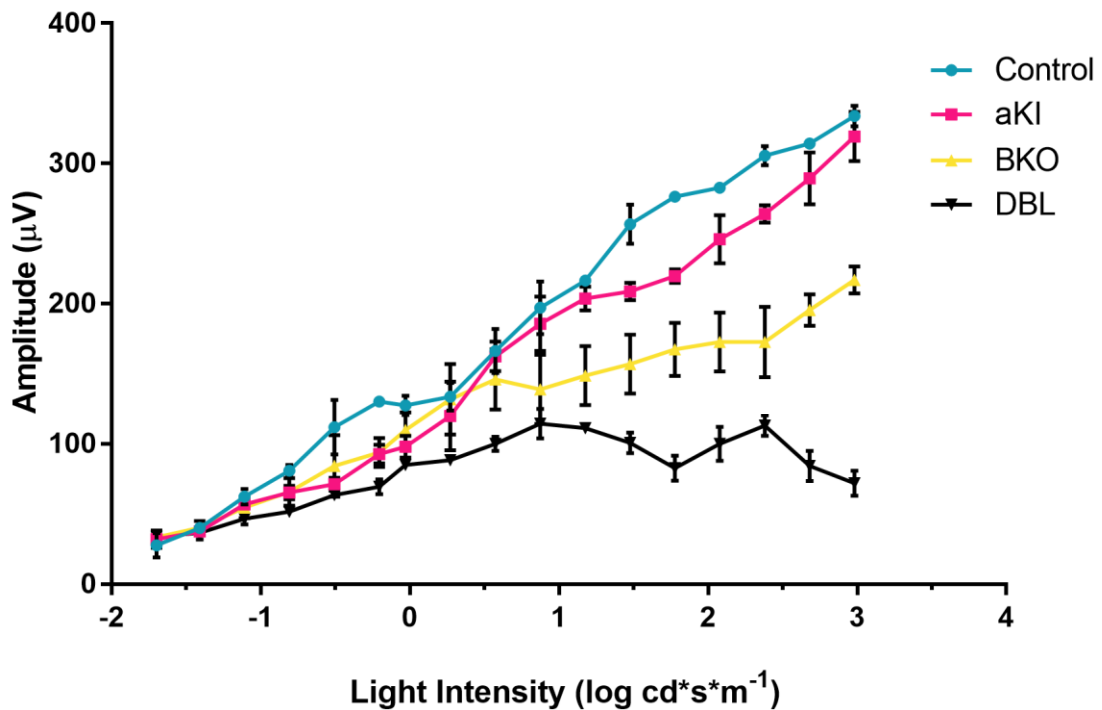


**Figure 18. B-wave amplitudes are attenuated in double conditional KO ERGs.** As flash intensities increased, the b-wave in control mice increases proportionately (blue) with flash intensity repeated measures yielding significantly different amplitudes ( $F_{16,128}=1626$ ,  $P<0.0001$ ).  $\alpha$ KI mice show a similar positive correlation between light intensity and b-wave amplitude (pink). At higher flash intensities, the b-wave amplitude in  $\beta$ KO mice continues to increase, but to a lesser extent than that of controls (yellow). Beginning at a flash intensity of  $0.875 \log \text{cd*s*m}^{-2}$ ,  $\beta$ KO b-wave amplitudes continue to be significantly different from controls ( $P<0.0001$ ). In DBL KO mice (black), the b-wave amplitude appears to hit a plateau at lower light intensity. The depolarization of cells in the inner retina, as measured by the b-wave, appear to be severely affected in the DBL KO when compared with all other mice studied. At a flash intensity of  $-1.108 \log \text{cd*s*m}^{-2}$ , the b-wave amplitude of the DBL KO mice is significantly different from controls ( $P<0.0003$ ) and continue to significantly deviate from control values at all increasing light intensities ( $P<0.0001$ ). (Mean  $\pm$  SD, 3 eyes for each group analyzed. Two-way repeated-measures ANOVA with Tukey's HSD post-hoc analysis between genotypes.).

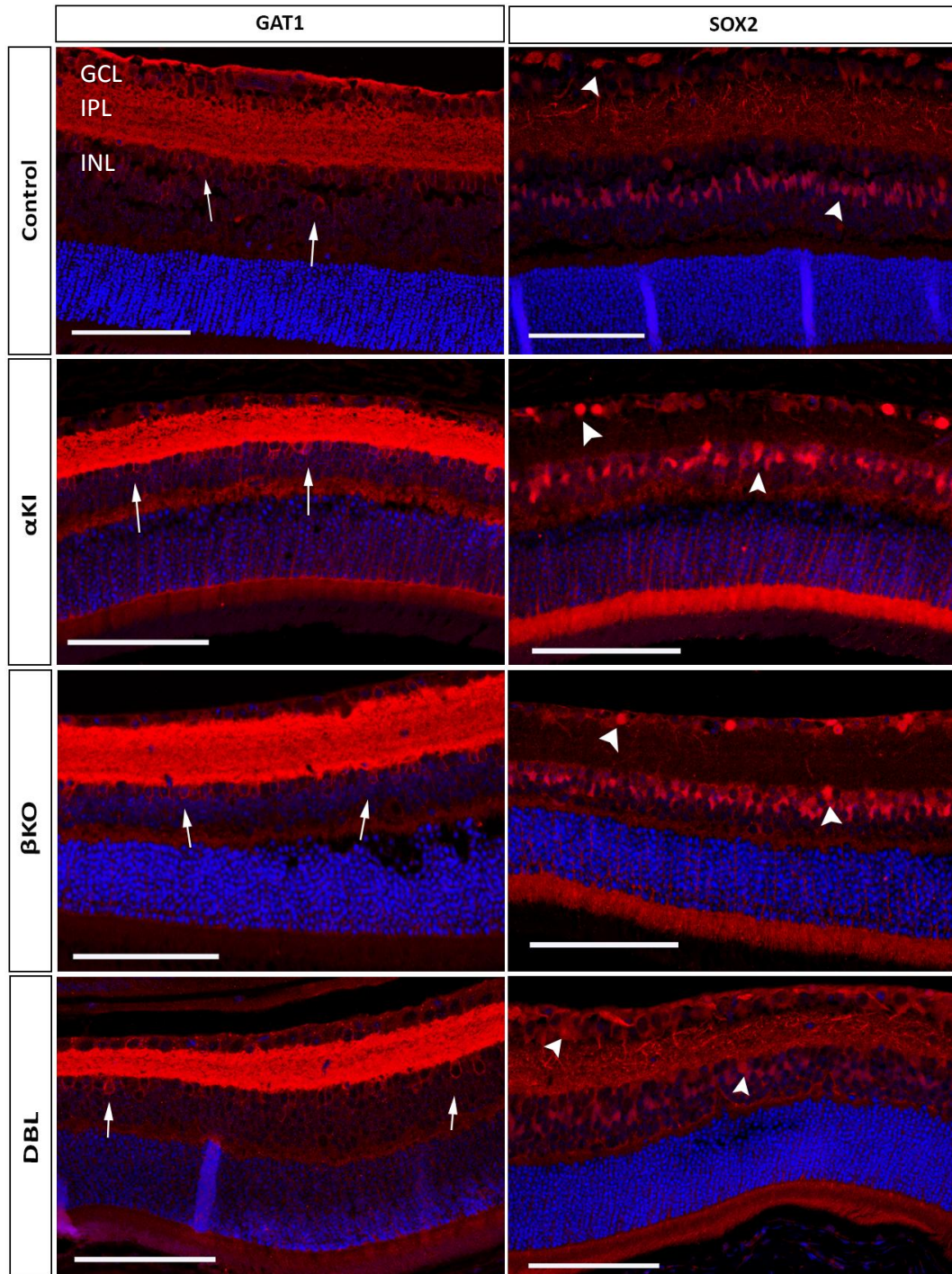


**Figure 19. Expression of GABAergic amacrine cell markers GAT1 and SOX2.** GAT1, a marker for GABAergic AC, showed similar membrane bound staining in all animals studied (arrows). SOX2, a marker for the cholinergic subset of GABAergic AC had similar expression in the conditional KO models to that seen in controls (arrowheads). Scale bars: 100µm.

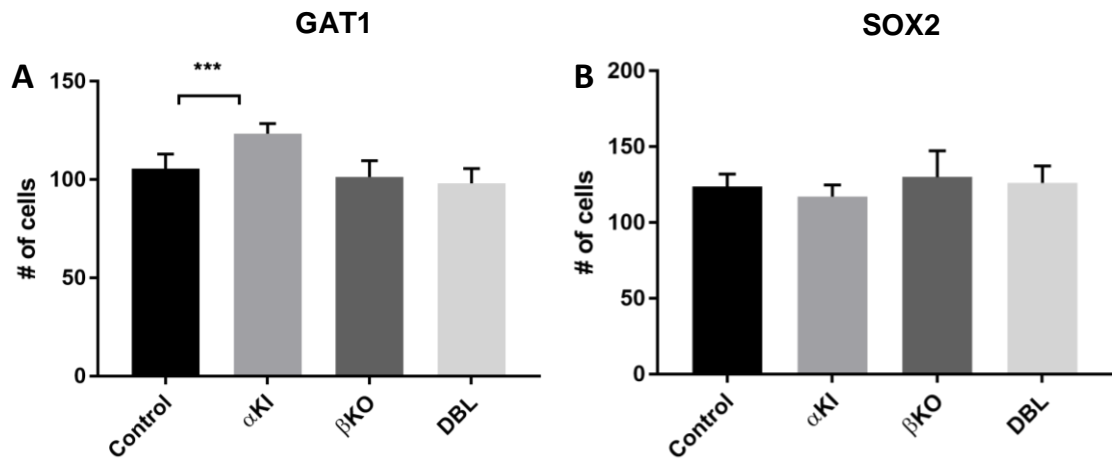


**Figure 20. GABAergic amacrine cells do not significantly decrease in AP-2 $\alpha$ /AP-2 $\beta$  conditional KOs.** (A) A significant increase in GAT1 positive cells was seen in  $\alpha$ KI mice ( $123 \pm 5.2$ ) compared to controls ( $106 \pm 7.4$ ). (B) No significant changes were seen in the number of SOX2-positive cells in any group ( $P > 0.05$ ). (Mean  $\pm$  SD for 3 retinas per group; \*\*\* $P < 0.0004$ , one-way ANOVA with Bonferroni multiple comparison tests).

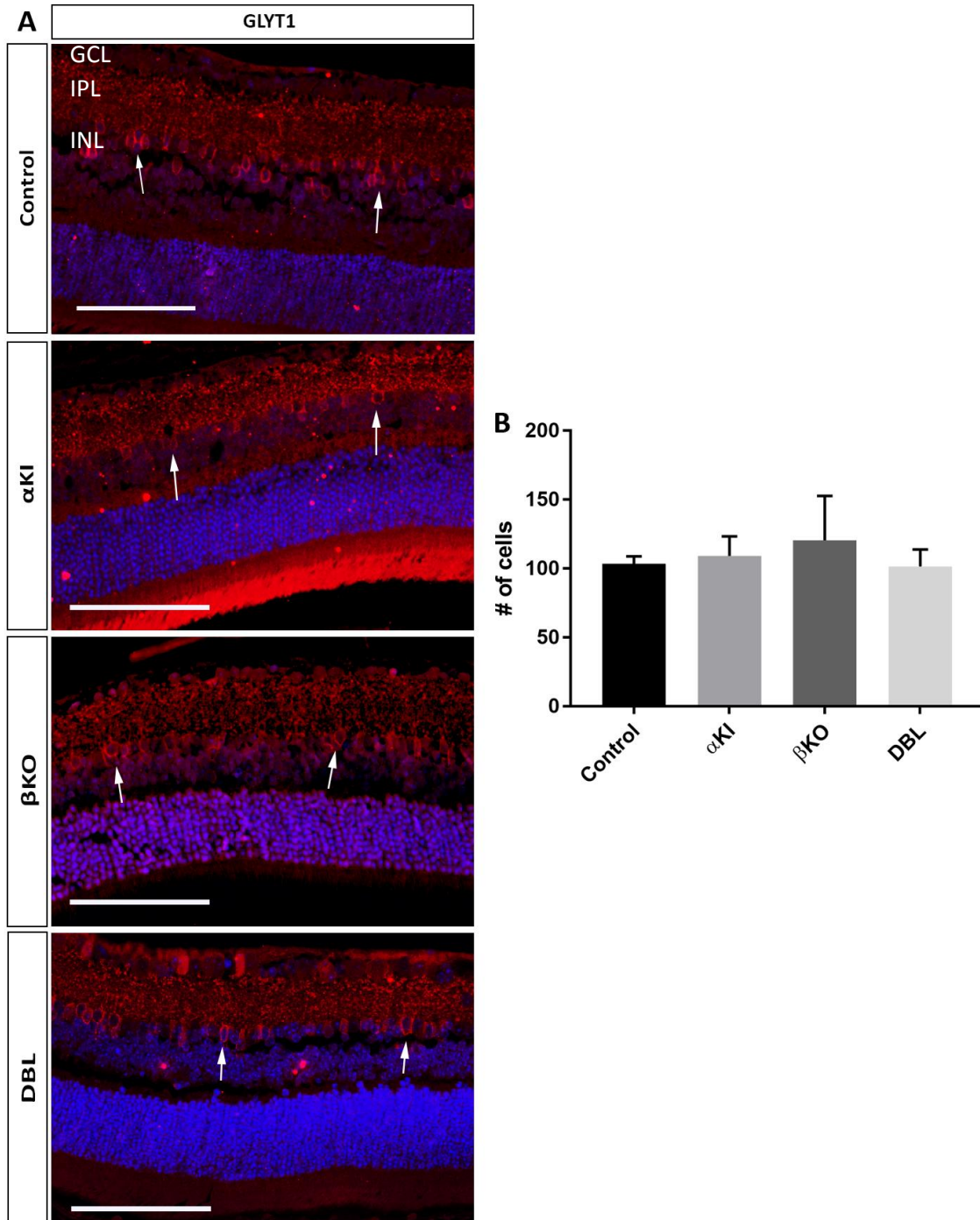


**Figure 21. Expression of the glycinergic amacrine cell marker, GLYT1.** (A) The expression of GLYT1 (red) in AC membranes (arrows) in the INL and GCL remains unchanged. (B) There is no significant difference in the number of these cells in AP-2 $\alpha$ , AP-2 $\beta$ , or AP-2 $\alpha$ /AP-2 $\beta$  knockout models (Mean  $\pm$  SD for 3 retinas per group;  $P > 0.05$ , One-way ANOVA). Scalebars: 100 $\mu$ m.

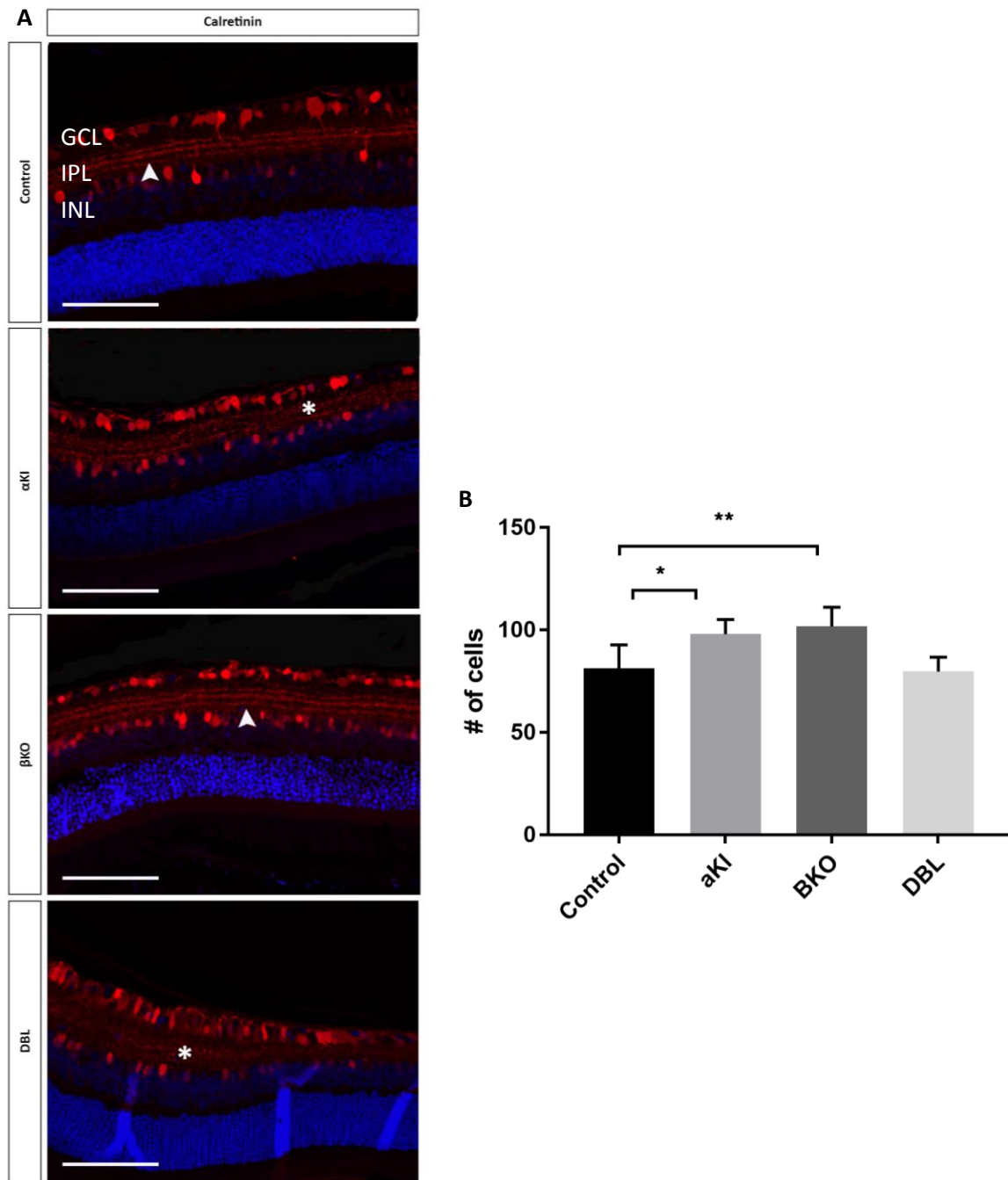


**Figure 22. Expression of Calretinin in knockout mice.** (A) The distinct pattern of three dendritic bands (arrowhead, control and  $\beta$ KO) are absent from the IPL of  $\alpha$ KI and DBL KO retinas (asterisk). (B) A significant increase in Calretinin-positive cells was seen in  $\alpha$ KI ( $98 \pm 7.1$ ) and  $\beta$ KO ( $102 \pm 9.2$ ) sections when compared with controls ( $81 \pm 11.2$ ). (Mean  $\pm$  SD for 3 retinas per group; \* $P < 0.017$ , \*\* $P < 0.0017$ , one-way ANOVA with Bonferroni multiple comparisons test). Scalebars: 100 $\mu$ m.